6672 J. Med. Chem. 2009, 52, 6672–6684
DOI: 10.1021/jm901013a

Journal of Medicinal Chemistry Article

Constrained Peptidomimetics Reveal Detailed Geometric Requirements of Covalent Prolyl Oligopeptidase Inhibitors

Janice Lawandi,[†] Sylvestre Toumieux,[†] Valentine Seyer,[†] Philip Campbell,[†] Sabine Thielges,[†] Lucienne Juillerat-Jeanneret,*[,‡] and Nicolas Moitessier*[,†]

[†]*Department of Chemistry, McGill University, 801 Sherbrooke Street W, Montréal, Québec, Canada H3A 2K6, and* [‡]*University Institute of Pathology, CHUV-UNIL, Rue du Bugnon 25, CH-1011 Lausanne, Switzerland*

Received July 9, 2009

Prolyl oligopeptidases cleave peptides on the carboxy side of internal proline residues and their inhibition has potential in the treatment of human brain disorders. Using our docking program FITTED, we have designed a series of constrained covalent inhibitors, built from a series of bicyclic scaffolds, to study the optimal shape required for these small molecules. These structures bear nitrile functional groups that we predicted to covalently bind to the catalytic serine of the enzyme. Synthesis and biological assays using human brain-derived astrocytic cells and endothelial cells and human fibroblasts revealed that these compounds act as selective inhibitors of prolyl oligopeptidase activity compared to prolyl-dipeptidyl-aminopeptidase activity, are able to penetrate the cells and inhibit intracellular activities in intact living cells. This integrated computational and experimental study shed light on the binding mode of inhibitors in the enzyme active site and will guide the design of future drug-like molecules.

Introduction

Prolyl oligopeptidase (POP,[a] EC 3.4.21.26) is a large (about 80 kDa), highly conserved, and widely distributed prolyl-selective serine endoprotease. Unlike other serine proteases, prolyl oligopeptidase can accommodate proline residues (and less frequently alanine residues) in its active site, cleaving short peptides on the carboxy side of these residues.[1] Over the last 15 years, abnormal POP activity, particularly in many regions of the brain,[2] has been linked to a number of diseases.[3−5] As a consequence, POP is believed to be a target for the treatment of neurodegenerative (e.g., Alzheimer's disease) and psychiatric (e.g., bipolar disorder[6]) disorders. A number of POP inhibitors, including covalent inhibitors such as Cbz-Gly-prolinal (**1**), Cbz-Pro-prolinal (**2**),[7] and JTP-4819 (**3**),[8,9] and noncovalent inhibitors (e.g., SUAM-1221 (**4**)[10] and S-17092-1 (**5**)[11]) have been prepared and evaluated in various experimental models. Some of these POP inhibitors were found to improve memory and learning[12] in animal models of brain disorders and to prevent amyloid-like depositions.[13−15] A few of these inhibitors also exhibited good pharmacokinetic and safety profiles and were able to penetrate the blood−brain barrier.[16] However, none has yet reached advanced clinical trials, and drug candidates are yet to be developed.

Although many POP inhibitors have been reported, a better understanding of the geometric and electronic requirements for a potent and selective POP inhibitor is still necessary in order to design improved POP inhibitors. Our aim in this study was not only to achieve selective inhibition of POP activity over other prolyl-specific proteases but also to reveal the optimal shape, size, and electronic requirement of a potent POP inhibitor. To reach these goals, we have exploited an approach integrating structures available from X-ray crystallography data, docking predictions, higher level computations (e.g., density functional theory, DFT), and chemical tools. We have combined and applied all of these techniques, also evaluating the inhibition of enzymatic activity, to reveal insight into binding and inhibition modes that each of them alone cannot predict. Using this strategy, we have designed a series of pseudopeptidic and peptidomimetic inhibitors, many of which are built around bicyclic scaffolds. These scaffolds closely mimic the known prolyl oligopeptidase inhibitor Cbz-Pro-prolinal (**1**, Figure 1).

We report herein docking predictions of a series of inhibitors into the active site of POP, followed by the synthesis and biological evaluation of the designed inhibitors in human cells. Of the entire series of compounds, one bicyclic scaffold exhibits high nanomolar inhibition of prolyl oligopeptidase activity and high selectivity over prolyl-dipeptidyl aminopeptidase activity in human brain astrocyte-derived cells, human brain-derived endothelial cells, and human fibroblasts. Combining results from the computational modeling and biological evaluation, optimal inhibitor geometry is revealed.

Results

Computer-Aided Design of Constrained Inhibitors. We combined structural knowledge from reported inhibitor structures, docking experiments, and evaluation of synthetic feasibility to design a series of inhibitors. To date, no crystal structure for the human isoform of prolyl oligopeptidase has been reported. However, a structure of POP from porcine brain (PDB code: 1H2Y), which demonstrates 97% identity

*To whom correspondence should be addressed. For N.M.: phone, 514-398-8543; fax, 514-398-3797; E-mail, nicolas.moitessier@mcgill.ca. For L.J-J.: phone, +41 21 314 7173; fax, +41 21 314 7115; E-mail: lucienne.juillerat@chuv.ch.

[a] Abbreviations: DFT, density functional theory; POP, prolyl oligopeptidase; DPP, dipeptidyl peptidase.

 Published on Web 10/12/2009

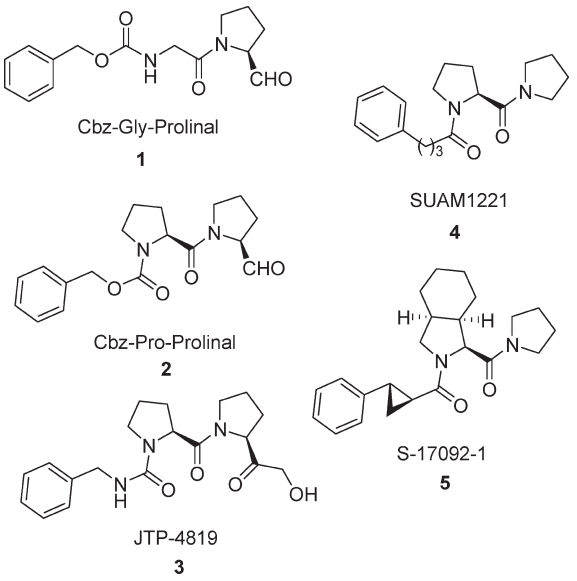

Figure 1. Selected POP inhibitors.

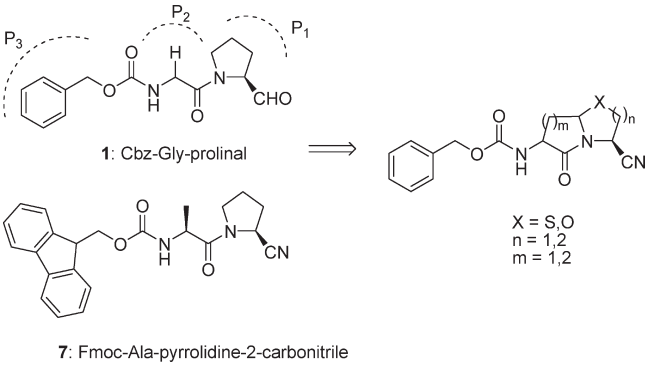

Figure 2. Pseudopeptidic inhibitors inspired from **1** and **7**.

with the human form, is available and can be used for docking experiments.[17]

As illustrated in Figure 2, this ligand-based design led us to the selected scaffold-based inhibitors, designed to mimic Fmoc-Ala-pyrrolidine-2-carbonitrile (**7**), previously shown to be a noncompetitive inhibitor selective for POP over DPP-IV,[18] and Cbz-Gly-prolinal (**1**). Several pieces of evidence[18] including a crystal structure of Cbz-Pro-prolinal bound to POP,[17] indicate that both inhibitors **1** and **7** are most likely reacting with the active site serine. For this work, we hypothesized that the designed inhibitors will also bind covalently to POP and covalent docking was carried out.

We used the latest version of our docking program FITTED (version 2.6)[19−21] to dock various covalent inhibitors, mainly built around rigid, bicyclic scaffolds. However, we first had to modify the program to perform covalent docking. With the novel implementations in the program, FITTED can now automatically identify reactive functional groups in the ligands (e.g., aldehydes, nitrile) and then dock these ligands, evaluating both the noncovalent and covalent binding modes simultaneously. As mentioned in the design section, we planned to develop constrained structures that would mimic pseudopeptidic inhibitors. The major interaction of these compounds is the covalent bond. However, the scoring of the binding of covalent inhibitors requires considering the reactivity of the reactive group (i.e., nitrile or aldehyde), which can vary significantly from one compound to another

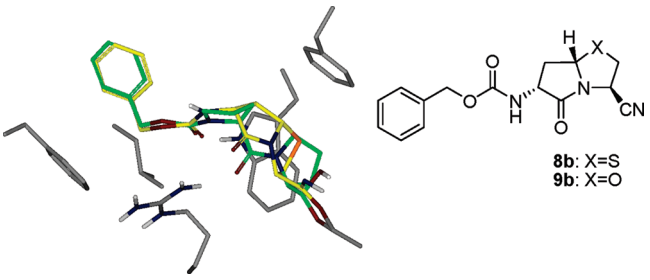

Figure 3. Docked designed covalent inhibitor (**8b**, green) overlaid with crystal structure of Cbz-Pro-prolinal (**2**, yellow).

as shown by Bayly and co-workers on a set of nitrile derivatives.[22] As the scoring of covalent bonds would require more advanced and much more time-consuming techniques to be accurate, our strategy cannot rely on generated scores. Instead we wished to design compounds that maintained the covalent bond and at least 2 of the 3 major interactions observed with these pseudopeptides. We have already successfully applied this strategy to the design of metalloenzyme inhibitors, as the metal coordination is not well scored either.[23]

Typically, a docking program used in conjunction with a scoring function predicting the binding affinity of the docked ligand gives high scores to good binders. However, none of the currently available scoring functions can handle covalent bonds formed upon docking. Thus, we visually inspected the docked poses, hypothesizing that if the bound pose retained the key interactions observed in the crystal structure, the docked ligand should be active. This assumption has been successfully exploited in other medicinal chemistry programs such as the development of nanomolar metalloprotease inhibitors.[23] Compound **2** binds to POP through two hydrogen bonds with the side chains of an arginine (Arg643) and a tryptophan (Trp595), while the five-membered ring proline ring sits on the aromatic ring of the Trp595 side chain. We predicted, using FITTED, that when bound to POP, the bicyclic structure **8b** should retain the key interactions made by **2** (Figure 3). We therefore prioritized **8b** for immediate synthesis. Synthetic routes enabling the synthesis of a small set of analogues of **8b**, with different ring sizes and heteroatoms, were developed. By varying only a few atoms of the bicyclic scaffold, small changes in geometry and chemical properties were calculated. For example, DFT calculations were carried out on the analogous scaffolds **8b** and **9b** and revealed significant differences in the electronic distributions, making the nitrile of **9b** less reactive (DFT results not shown).

To evaluate the impact of the conformational constraint of the bicyclic structures, we also designed and prepared a series of pseudopeptides, closely resembling the bicyclic scaffolds, in order to compare the bioactivity of the flexible dipeptide to that of the corresponding rigid bicyclic scaffolds. From the docking study, we predicted that the five-membered proline ring of compounds **11a** and **12a**,**b** sits on the aromatic side chain of Trp595. Our docking studies also indicated that this interaction should be disrupted when a six-membered ring (**14**) is introduced; a loss of potency is expected. We chose to also synthesize **14** and test it to validate our docking predictions.

Chemistry

Synthesis of the Pseudopeptidic Inhibitors. The series of pseudopeptides, incorporating either a piperidine-2-

Scheme 1[a]

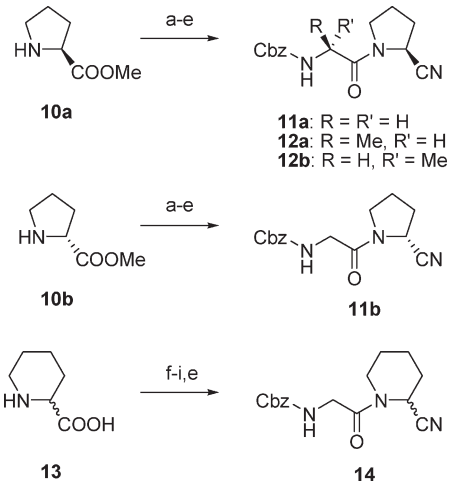

[a] (a) Boc_2O, Et_3N, DMAP, CH_2Cl_2, 40%; (b) NH_3 (aq) 28%, THF, 60°C, 89%; (c) $(CF_3CO)_2O$, Et_3N, THF, 0 °C, 74−83%; (d) CF_3CO_2H, CH_2Cl_2, 0°C, 29−53%; (e) RCOOH (Cbz-Gly-OH or Cbz-Ala-OH or Cbz-D-Ala-OH), Et_3N, HOBt, EDCI, CH_2Cl_2, 30−65%; (f) Boc_2O, Et_3N, 1,4-dioxane/H_2O, 82%; (g) $ClCO_2Et$, Et_3N, THF, −15°C then NH_3 (aq) 28%, rt, 83%; (h) $(CF_3CO)_2O$, Et_3N, CH_2Cl_2, 0 °C, 52−68%; (i) HCl, 1,4-dioxane, 90%.

carbonitrile or pyrrolidine-2-carbonitrile moiety, was synthesized as described in Scheme 1. To synthesize Cbz-Gly-L/D-pyrrolidine-2-carbonitrile (**11a**,**b**) and Cbz-L/D-Ala-L-pyrrolidine-2-carbonitrile (**12a**,**b**), the pyrrolidine nitrile portions were prepared from L- and D-Pro methyl esters using previously reported procedures (see Experimental Section). Then the carbonitrile derivatives were coupled to Cbz protected Ala and Gly residues. In parallel, we also prepared the racemic compound **14** from pipecolinic acid **13**. The procedures used to prepare the pyrrolidine-2-carbonitriles were not as successful on pipecolinic acid **13**. We therefore used slightly different methods to make **14** (listed in steps f−i of Scheme 1).

Synthesis of the Bicyclic Scaffolds. Following the synthesis of the pseudodipeptides, we synthesized the (5,5) fused scaffolds as enantiopure compounds or diastereomeric mixtures enriched in the diastereomer that we predicted to be most active from the docking and the initial results from the biological testing (Scheme 2).[24−28] After protection of the amine and acid functions of allyl Gly *rac*-**15**,[29] we oxidized the alkene to the corresponding aldehyde *rac*-**16** in quantitative yields.[30] Reaction of this aldehyde (*rac*-**16**) with L-Cys-OMe at room temperature, and then at 50 °C for several days in pyridine, afforded the first two bicyclic structures **17a** and **17b** after careful chromatographic separation. Alternatively, we repeated this same procedure to prepare the desired bicyclic structures **17c** and **17d** as a separable 1:1 diastereomeric mixture. The same approach was applied to other amino acids, and we synthesized the scaffolds **18a** and **18b** from *rac*-**16** and L-Ser-OMe and **19a** and **19b** from *rac*-**16** and L-Thr-OMe.

To probe the geometric requirement for optimal binding and to probe the computational predictions, the size of the right-hand five-membered ring was expanded to **20** as a mimic of **14**. *rac*-**20** was prepared following synthetic routes similar to the one used previously (Scheme 2). In contrast to the synthesis of the 5,5-bicyclic structures, none of the other possible diastereomers were isolated in a large enough amount to enable any further transformations. In addition,

Scheme 2[a]

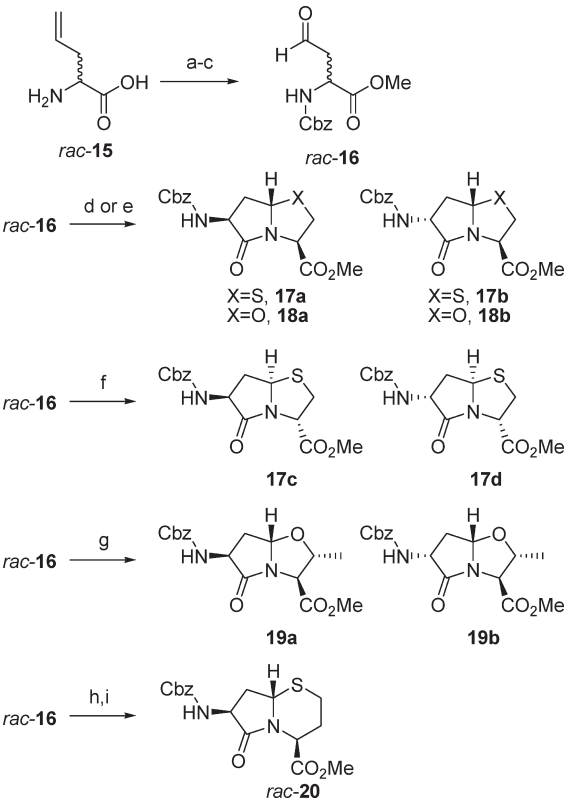

[a] (a) TMSCl, MeOH, 0 °C to rt; (b) CbzCl, Et_3N, 0 °C; (c) O_3, CH_2Cl_2, then DMS; (d) L-Cys-OMe, pyridine, molecular sieves, then pyridine, 50 °C, 4 days, 48% **17a**,**b** (over 3 steps); (e) L-Ser-OMe, pyridine, molecular sieves, then pyridine, 50 °C, 4 days, 49% of **18a**,**b** (over 3 steps); (f) (i) D-Cys-OH, pyridine, molecular sieves, then pyridine, 50 °C, 4 days, (ii) $TMSCHN_2$, CH_2Cl_2 33% of **17c**,**d** (over 4 steps); (g) L-Thr-OMe, pyridine, molecular sieves, then pyridine, 50 °C, 4 days, 35% of **19a**,**b** (over 3 steps); (h) L-homo-Cys-OH, pyridine, 50 °C, 4 days; (i) $TMSCHN_2$, CH_2Cl_2, 32% of *rac*-**20** (over 4 steps).

Scheme 3[a]

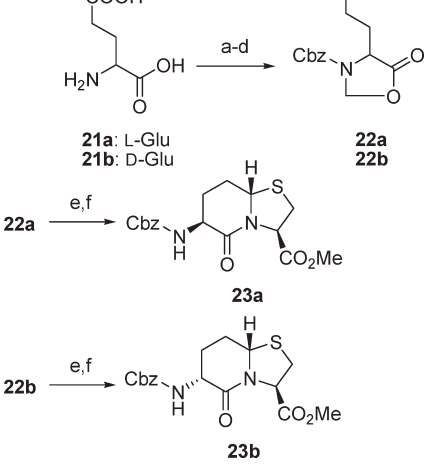

[a] (a) CbzCl, 4 N NaOH, 0 °C to rt, 21 h; (b) $(CH_2O)_n$, cat. pTsOH, toluene, reflux, 3h; (c) $(COCl)_2$, cat. DMF, CH_2Cl_2, quant; (d) LiAl[OtBu]$_3$H, THF; (e) (i) L-CysOMe·HCl, pyridine, 24 h, (ii) 50 °C, 3 days; (f) K_2CO_3, MeOH, 6−8% over 6 steps.

our docking studies predicted a distorted binding mode and further efforts to make the other isomers were deemed unnecessary.

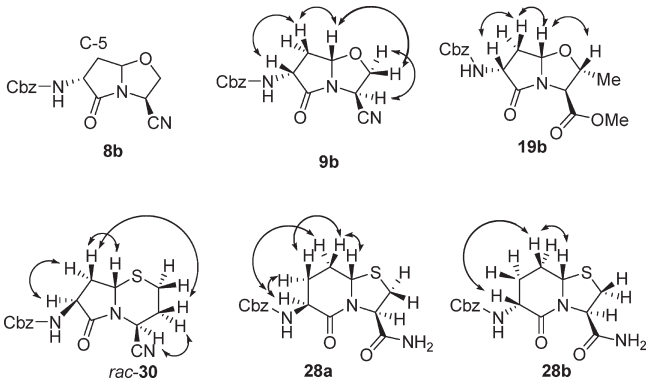

Figure 4. Selected NOE identifying the stereochemistry of the isolated compounds.

Scheme 4[a]

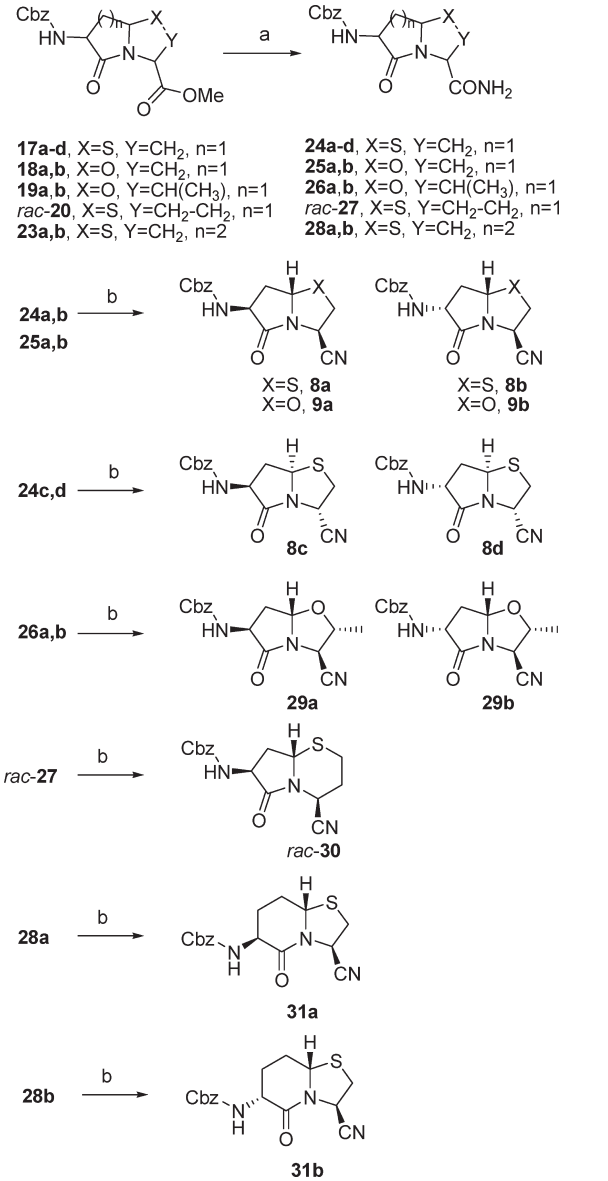

[a](a) NH_3, MeOH, rt, quant; (b) $(CF_3CO)_2O$, Et_3N, THF, rt, 27−81%.

Two additional diastereomeric scaffolds (**23a** and **23b**) were prepared from L- and D-Glu (**21a**,**b**) using a modified strategy reported by Subasinghe et al.[26] This strategy relies on the intermediate **22**, which upon treatment with L-Cys-OMe afforded the desired structure in a single step (Scheme 3).

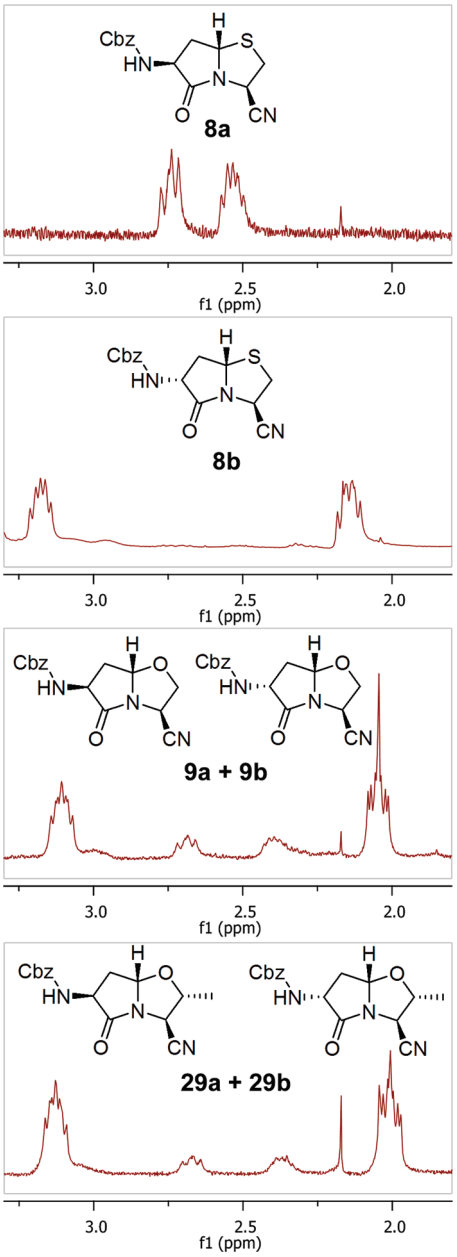

Figure 5. Comparison of ^{1}H NMR spectra, confirming stereochemistry of isolated diastereomers. The peaks refer to the two hydrogen atoms on carbon no. 5 (see **8b** in Figure 4).

Functionalization of the Scaffolds to Covalent Inhibitors. The covalent functionality was added to each of the scaffolds once formed (Scheme 4). For this purpose, we converted each of the methyl esters into the corresponding amides, **24a** through **28b**, using ammonia,[31] which we then transformed into the corresponding nitriles with good to excellent yields by dehydration.[32]

Confirming the Stereochemistry of the Various Diastereomers. Given that **17a**−**d** are reported in the literature,[25,33] providing stereochemistry identified by NOE experiments, we compared NMR data from our purified compounds to the reported data. For all other bicyclic compounds, both COSY and NOESY experiments were performed to identify

Table 1. Inhibition of POP Activity and DPP-IV Endoprotease Activity in Cell Extracts

	Z-Gly-Pro-AMC (POP activity)[a]			Gly-Pro-AMC (DPP IV activity)[a]		
compd	human astrocyte-derived cells [b]	human brain-derived endothelial cells[c]	human fibroblasts[d]	human astrocyte-derived cells	human brain-derived endothelial cells	human fibroblasts
Z-Pro-NH_2	+	−	+	−	−	−
Z-Pro-CN	−	+	−	−	−	−
Boc-Pro-CN	−	−	−	−	−	−
Pro-CN	−	−	−	−	−	nd
11a	+++	+++	+++	−	−	−
11b	+++	+++	+++	−	−	−
12a	+++	+++	+++	−	−	−
12b	+++	+++	+++	−	−	−
14	++	+	+	−	−	−
17a	+	−	+	−	−	−
17b	−	−	+	−	−	−
24a	−	−	−	−	−	−
24b	−	−	−	−	−	−
8a	+	++	+	−	−	−
8b	+++	+++	+++	−	−	−
8c	+	+	−	−	−	−
8d	+	++	+	−	−	−
9a,b	−	−	+	−	−	−
29a,b	+	+	−	−	−	−
rac-**30**	−	−	+	−	−	−
31a	++	++	++	−	−	−
31b	++	++	++	−	−	−

[a] −, No inhibition at 100 μM; +, 10−50% inhibition at 100 μM; ++, >50% inhibition at 100 μM; +++, >90% inhibition at 20 μM; nd, not determined. [b] LN18, LN229, LNZ308: human glioblastoma cells. [c] HCEC, human brain-derived endothelial cells. [d] PO03, human lung-derived fibroblasts; PG98/5, human skin-derived fibroblasts.

the isolated diastereomers (Figure 4). In addition, only one stereogenic center is made throughout the synthesis while the other two already appear in the starting amino acids. When racemic allyl glycine was used, two stereogenic centers needed to be assigned.

To further confirm the stereochemistry of the scaffolds, we simply compared the ^{1}H NMR spectra of the novel scaffolds to those of **8a**−**b** (Figure 5).

Biological Evaluations

Enzyme Inhibition in Cell Extracts. POP activity was measured using the fluorogenic substrate Z-Gly-Pro-AMC and prolyl-dipeptidyl-aminopeptidase (DPP IV) activity with the fluorogenic substrate Gly-Pro-AMC using the human brain astrocyte-derived LN18, LN229, and LNZ308 glioblastoma cells, the human brain-derived HCEC endothelial cells and the human lung-derived PO03 and skin-derived PG98/5 fibroblasts. The initial inhibition screening experiments were performed using cell extracts, obtained by extracting cell layers in PBS-0.1% Triton X-100 to determine the potential of the developed inhibitors to inhibit total cellular enzyme activities (Table 1).

All compounds were found to be very selective for POP activity over DPP IV activity in cell extracts.

Enzyme Inhibition in Intact Living Cells. To evaluate the potential of these molecules to inhibit membrane-inserted enzymes as well as to penetrate cells and inhibit intracellular enzymatic activities, the inhibition of POP activity was also evaluated with the same compounds in intact living cells (Table 2).

As shown in Table 2, the inhibitors not only inhibit POP activity in cell extracts but also this proteolytic activity in intact living cells. Out of all the compounds tested, compounds **11a**, **11b**, **12a**, **12b**, and **8b** were the best inhibitors of POP activity. To obtain more detailed information concerning the potency of **11a**, **11b**, **12a**, **12b**, and **8b** as POP inhibitors, the IC_{50} values were determined in cell extracts and in intact cells (Figure 6 and Table 3).

Table 2. Inhibition of POP Endoprotease Activity in Intact Living Cells

	Z-Gly-Pro-AMC (POP activity)[a]		
compd	human astrocyte-derived cells	human brain-derived endothelial cells	human fibroblasts
Z-Pro-NH_2	+	−	−
Z-Pro-CN	−	−	+
Boc-Pro-CN	−	−	−
Pro-CN	−	−	−
11a	+++	+++	+++
11b	+++	+++	+++
12a	+++	+++	+++
12b	+++	+++	+++
14	+	−	−
17a	−	−	+
17b	−	−	+
24a	−	−	−
24b	−	−	−
8a	−	+	+
8b	+++	+++	+++
8c	−	−	−
8d	−	+	−
9a,b	−	−	+
29a,b	−	+	−
***rac*-30**	−	−	−
31a	++	+	++
31b	++	++	++

[a] −, No inhibition at 100 μM; +, 10−50% inhibition at 100 μM; ++, >50% inhibition at 100 μM; +++, >90% inhibition at 20 μM.

Compounds **12a** and **11a** are the most potent inhibitors of POP activity of our series, displaying low nanomolar IC_{50} values. They are also very selective over DPP IV activity, both in cell extracts and in intact cells (data not shown). The inhibition of POP activity, as defined by IC_{50}, is about

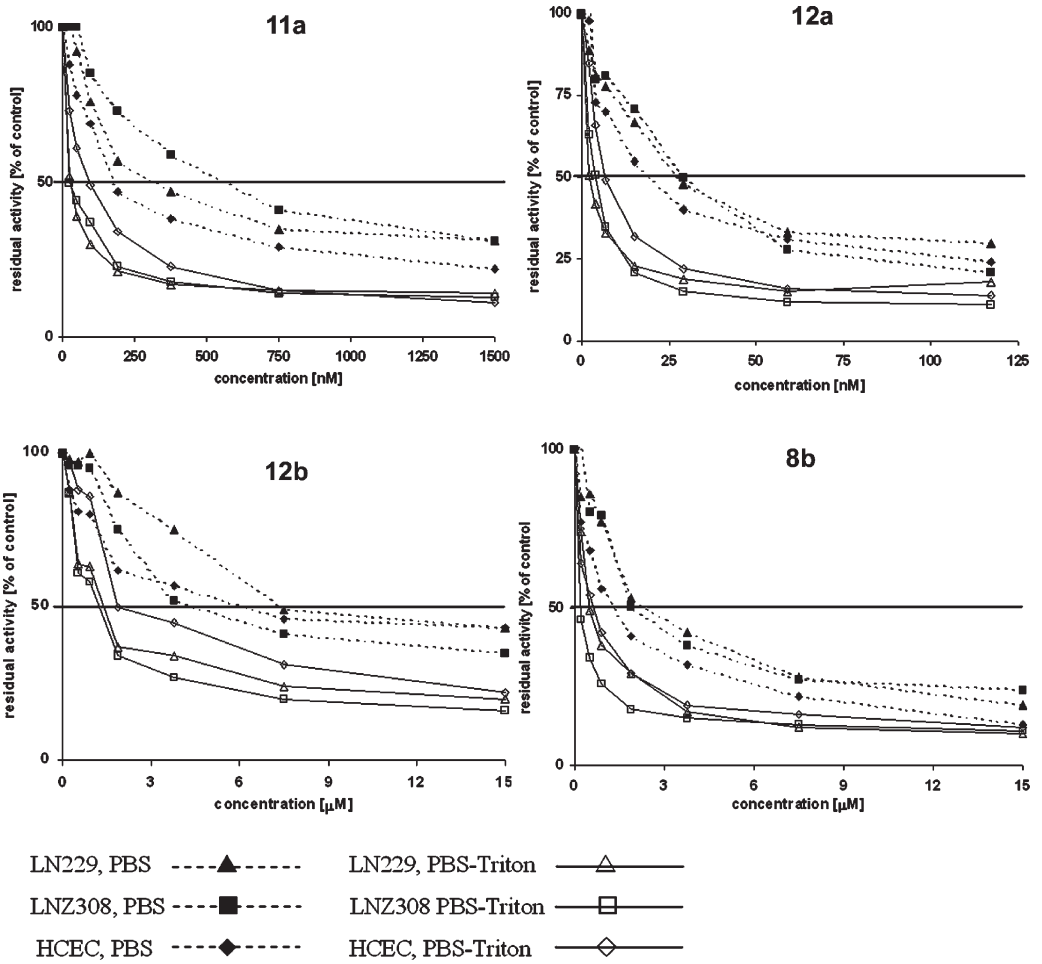

Figure 6. Dose−response inhibition of POP activity by **11a**, **11b**, **12a**, **12b**, and **8b** in intact cells (PBS) and in cell extracts (PBS-Triton).

10-fold higher in cell extracts than in intact cells, possibly reflecting the partial efficacy of these inhibitors of crossing the cell membrane.

Discussion

POP and Other Prolyl Peptidases. The family of serine peptidases able to cleave peptide bonds after a prolyl residue comprises exopeptidases such as the cell plasma-membrane anchored DPP IV/CD26 and FAP-α/seprase, and the intracellular DPP8, DPP9, and endopeptidases, mainly represented by the widely distributed intracellular prolyl oligopeptidase (POP). POP and/or POP-like activity have been found in many regions of the brain[2,34] and has been associated with the cleavage of oligopeptides involved in memory and the processing of amyloid precursor protein to β-amyloid.[15] Studies on animal models suggested that POP inhibition may lead to improved memory and learning in rodents,[13,35] to reverse scopolamine-induced amnesia in rats,[36] and to enhance cognition in Parkinson's disease.[37] Human POP levels are reduced in different stages of depression, increased in maniac and schizophrenic patients, and the enzyme is reactivated to normal levels by antidepressants.[38] Conflicting data regarding altered POP activity[13,39] have been reported in patients with Alzheimer's disease. Thus, POP activity may represent a target for the treatment of neurological disorders. However, FAP-α/seprase, and possibly the DPP8/DPP9 proteases, also display postprolyl hydrolytic endoproteolytic activities.[34] Therefore, several proteases may share the endoproteolytic activity attributed to POP. Highly specific POP inhibitors therefore need to be designed in order to further explore this enzyme and its function.

As our long-term aim is to develop POP inhibitors targeting POP expressed in the brain, and as most of the information concerning POP and its inhibitors was obtained in brain models, we evaluated the inhibitory potency of our compounds in human brain-derived cells of astrocytic origin (glioblastoma cells) and endothelial cells as a model of cells forming the blood−brain barrier. As POP and POP activity are widely expressed in many other cells, we also evaluated the inhibitory potential of the inhibitors in human fibroblasts of the lung or the skin, as models for non-brain-derived cells. Selectivity for endoproteolytic POP activity over exoproteolytic DPP IV activity can easily be obtained due to the different chemical properties of their catalytic site (DPP IV binds to charged terminal residues while POP does not). Selectivity for other prolyl-specific endoproteolytic activities is challenging and in fact rarely reported.[40]

Constrained POP Inhibitors. In contrast to noncovalent competitive inhibitors which can adjust their orientation and translation in the enzyme binding site, the orientation of covalent inhibitors is tightly controlled by the forming covalent bond and any seemingly minor change in shape can have a significant impact on the binding affinity. The docking study and biological testing of the scaffold-based structures revealed **8a** and **8b** as potent POP inhibitors. The biological evaluation of the analogues provided more in

Table 3. IC_{50} Values [nM] for the Inhibition of POP Endoproteolytic Activity in Intact Living Cells and in Cell Extracts

	LN229 (nM)		LNZ308 (nM)		HCEC (nM)	
compd	intact cells	cell extract	intact cells	cell extract	intact cells	cell extract
11a	325	20	590	20	180	95
11b	3400	430	>4000	430	2800	690
12a	28	3	29	5	20	7
12b	7500	1400	4700	1200	6600	2000
8b	2000	500	2500	200	1300	700

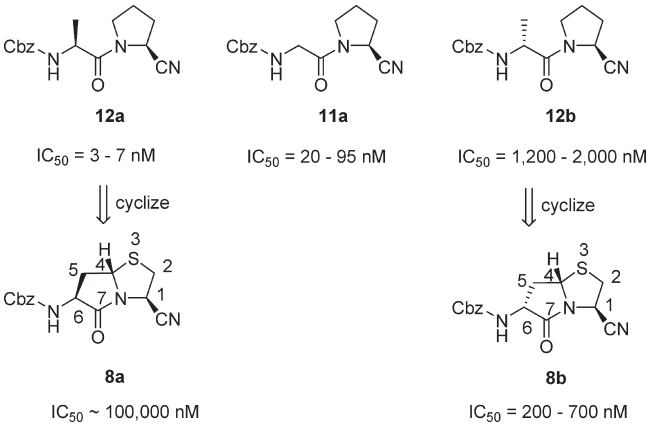

Figure 7. Effect of cyclization on inhibitory potency.

depth information about the required functional groups and stereochemical features of the inhibitors. First, comparing **8a**/**b** to **17a**/**b** and **24a**/**b** revealed that the nitrile functional group is essential for optimal binding, most likely through the postulated covalent bond with the catalytic serine. Then the predicted drop in activity observed from **11a** to **14** and from **8a** to *rac*-**30** confirmed that mimicking the Pro ring of Cbz-Gly-prolinal (**1**) with a larger ring results in loss of binding affinity. Unlike with the five-membered ring systems mimicking Pro, this expanded six-membered ring cannot fit into the binding site without clashing with the enzyme or disrupting the key hydrogen bonds and hydrophobic interactions. The bound pose is distorted when compared to the crystal structure, as revealed by our docking studies.

Furthermore, the replacement of the sulfur atom of **8b** by an oxygen atom (in **9b**) resulted in a complete loss of activity. Although reduction in inhibitory potency has been observed when moving from thiooxazoline to oxazoline,[41] such a large drop in affinity is unexpected. Again, we hypothesize that these changes are magnified by the fact that these inhibitors bind covalently. This seemingly subtle change actually leads to reduced ring size, C−S bonds being significantly longer than C−O bonds. As for *rac*-**30**, the increase to a six-membered ring resulted in a different shape of the whole molecule, hence a different binding affinity. To further probe the differences between these two structures, DFT calculations were carried out and revealed a significantly different electronic distribution and a much less polarized (i.e., less reactive) nitrile group in **9b** when compared to **8b**. This reduced reactivity may prevent the covalent binding.

The stereochemistry of the molecular scaffolds was also critical for the inhibition of POP endoproteolytic activity (**8a** vs **8b**, **8c**, or **8d**). As expected, the natural amino acid configuration is required at the nitrile position (**8a** vs **8c**, **8b** vs **8d**, or **11a** vs **11b**) in order to mimic the natural Pro-containing substrate of the enzyme. More interestingly, the optimal configuration of the left-handed stereogenic center

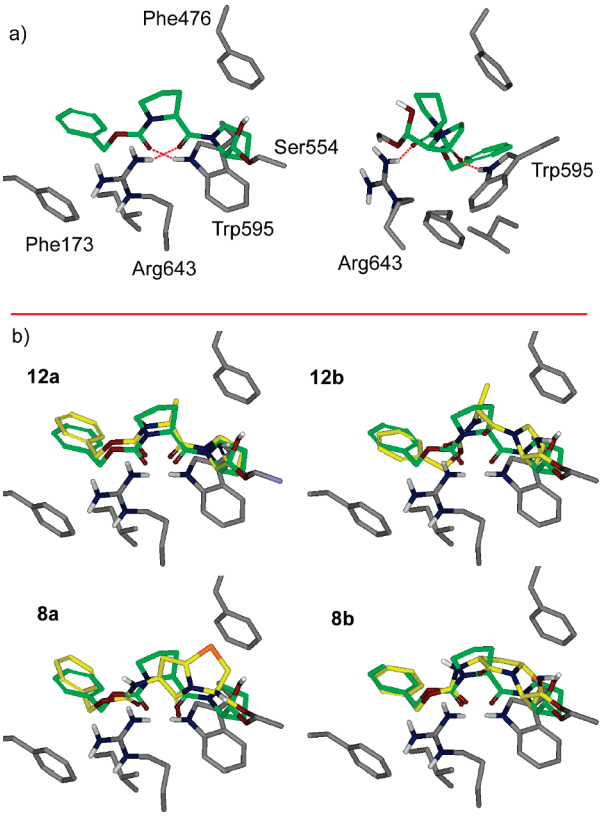

Figure 8. (a) Structure of Cbz-Pro-prolinal cocrystallized with POP. (b) Docked structures of **12a**, **12b**, **8a**, and **8b** (yellow) superposed to the crystal structure of Cbz-Pro-prolinal (green).

(carbon 6 in Figure 7) of the scaffold mimics the D-amino acid configuration (**8a** vs **8b**). To investigate this specific observation, we prepared the corresponding pseudopeptides **12a** and **12b** (Figure 7). When moving from Gly to L-Ala (**11a** to **12a**), the inhibition increased by an order of magnitude. More interestingly, when the configuration of the Ala residue was inverted (**12a** to **12b**) (Figure 7), inhibition was still observed but dropped by a factor of 500. Similarly, when the Pro stereogenic center is inverted, **11a** versus **11b**, inhibition is observed, although with a higher IC_{50} for the D-isomer. This data suggests that the stereochemistry at these two centers have an impact on the potency.

As shown in Figure 8, the proposed binding mode of **12a** is very similar to the experimentally observed binding mode of Cbz-Pro-prolinal. The proline ring stacks on Trp595 and interacts with Phe476, while the terminal phenyl ring interacts with Phe173 and the two hydrogen bonds between carbonyls of the inhibitor and the enzyme are retained. In contrast, **12b** does not fit as nicely in the binding site and a hydrogen bond is lost, resulting in a significant drop in potency. When constraining **12a** and **12b** into **8a** and **8b**, a loss of activity is observed from **12a** to **8a**, while a slight

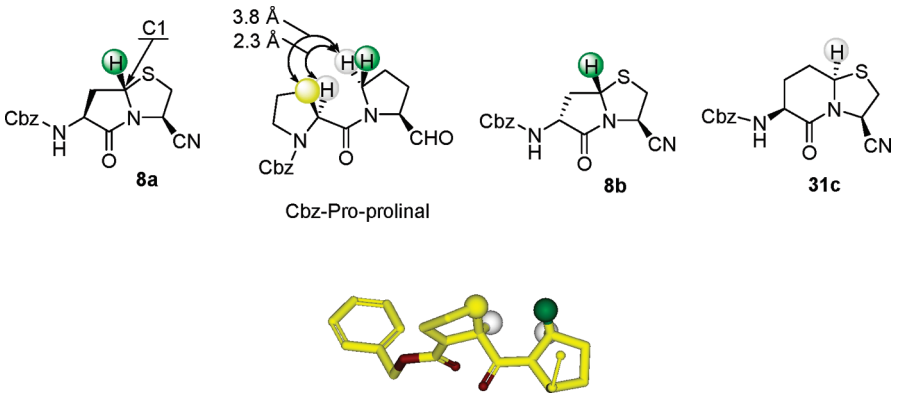

Figure 9. Effect of cyclization on inhibitory potency.

increase is observed from **12b** to **8b**. We rationalize that the stereochemistry of the carbon C1, which is imposed by the synthetic pathway influences the binding (Figures 8 and 9). Comparing the crystal structure of Cbz-Pro-prolinal, cocrystallized with POP (PDB code: 1H2Y), and the docked conformations of **12a**, **12b**, **8a**, and **8b**, shows that, when compared to **8a**, **8b** adopts a shape that more closely replicates the interactions of the enzyme with Cbz-Pro-prolinal (Figure 8). This observation is consistent with the measured inhibitory potencies of these inhibitors on POP, where we noted that **8b** was more potent than all the other bicyclic structures. Interestingly, the binding mode and more specifically of the position of the proline ring of **12b** and **8b** are fairly similar while the binding mode of **12a** and **8a** are quite different as are the measured potencies. In practice, the cyclization of **12b** corresponds to the substitution of the two hydrogen atoms highlighted by gray spheres of Cbz-D-Pro-prolinal in Figure 9 by a covalent bond and to the production of **8b**. In contrast, the proline β-carbon (shown in yellow) is not positioned to be covalently linked to the γ-carbon of the Cbz-L-Pro-prolinal. As a result, when **12a** is cyclized into **8a**, **8a** cannot adopt the bioactive conformation of **12a**.

Further docking studies with **31c**, an epimer of **31a**, revealed that the binding mode should be very similar to Cbz-Pro-prolinal and **31c** is therefore expected to be a tight binder. Unfortunately, all our synthetic efforts to make **31c** proved unsuccessful. This last observation will now guide our future synthetic efforts to make constrained bicyclic POP inhibitors.

POP Activity and Selectivity in Intact Cells. The inhibitory potency of these compounds was maintained in intact living cells (Table 2). These experiments demonstrate that the developed inhibitors are penetrating the cells, a key feature if POP inhibitors have to be efficient as therapeutic agents for neurodegenerative diseases because their target enzyme is intracellular. Moreover, when assessed for inhibition toward DPP IV activity, none of the compounds exhibited inhibitions at concentration as high as 100 μM. This data clearly demonstrates the high selectivity of **8a** and **8b** for POP activity.

Overall, these molecules achieved excellent selectivity for inhibition of POP endoproteolytic activity over inhibition of DPP IV exoproteolytic activity in soluble enzyme activities extracted from relevant cell models and in human intact living astrocyte-derived cells, human brain-derived endothelial cells, and human primary fibroblasts.

Conclusion

We have used a series of constrained peptidomimetics to better understand some important inhibitor shape requirements leading to more potent inhibitors of prolyl oligopeptidase. We first used a novel feature of our docking program FITTED to dock covalent inhibitors to the binding site of prolyl oligopeptidase and to select a lead scaffold for synthesis. On the basis of this docking study, two were selected for synthesis (**8a** and **8b**). To validate our predictions, several analogues of different sizes, stereochemistry, and shapes were also prepared. Exhaustive biological evaluation confirmed our prediction and identified **8b** as a potent, highly selective, and cell-permeant POP inhibitor (IC_{50} of 200−700 nM). Through this series of seemingly similar compounds, we demonstrated that scaffolding is very sensitive to seemingly subtle changes such as the substitution of a sulfur atom by an isosteric oxygen atom. The docking studies also identified the configuration of the stereogenic center at the ring junction as a limiting factor for optimal activity and will lead our design of the second generation of more potent inhibitors.

Experimental Section

Synthesis. All commercially available reagents were used without further purification unless otherwise stated. 4 Å molecular sieves were dried at 100 °C prior to use. Optical rotations were measured on a JASCO DIP 140 in a 1 dm cell at 20 °C. FTIR spectra were recorded using a Perkin-Elmer Spectrum One FT-IR. ^{1}H and ^{13}C NMR spectra were recorded on Varian Mercury 400 MHz, 300 MHz, or Unity 500 spectrometers. Chemical shifts are reported in ppm using the residual of chloroform as internal standard (7.26 ppm for ^{1}H and 77.160 ppm for ^{13}C, respectively). Thin layer chromatography visualization was performed by UV or by development using $KMnO_4$, H_2SO_4/MeOH or Mo/Ce solutions. Chromatography was performed on silica gel 60 (230−40 mesh). Low resolution mass spectrometry was performed by ESI using a Thermoquest Finnigan LCQDuo. High resolution mass spectrometry was performed by EI peak matching (70 eV) on a Kratos MS25 RFA double focusing mass spectrometer or by ESI on a IonSpec 7.0 T FTMS at McGill University. Prior to biological testing, reversed phase HPLC was used to verify the purity of compounds on an Agilent 1100 series instrument equipped with VWD-detector, C18 reverse column (Agilent, Zorbax Eclipse XDB-C18 150 mm × 4.6 mm, 5 μm), UV detection at 254 nm. All measured purities are listed in Table 4 in the Experimental Section "HPLC Analysis of Purity." All tested compounds were ≥95% pure, except for compounds **14**, **17a**, and **24b** (≥90% pure), which were not active according to our biological tests.

(2*S*)-*N*-(*tert*-Butoxycarbonyl)proline Methyl Ester.[42] To a solution of L-proline methyl ester hydrochloride (1.00 g, 6.06 mmol) in 10 mL of dry CH_2Cl_2 was added Boc_2O (2.90 g, 13.3 mmol), Et_3N (0.92 mL, 6.61 mmol), and DMAP (0.81 g, 6.64 mmol) at 0 °C under Ar. After 18 h, the crude mixture was washed with aqueous HCl 0.5 M, saturated aqueous $NaHCO_3$ solution, H_2O, and brine. The organic phase was dried over

Table 4. HPLC Analysis of Purity

compd	analysis condition	retention time (min.)	purity (%)
11a	B	4.3	98.7
11b	B	4.5	98.8
12a	B	5.9	98.0
12b	B	5.7	98.2
14	B	8.7	92.5
17a	A	3.8	91.9 (9:1 of **17a**:**17b**)
17b	A	3.3	96.7 (1:9 of **17a**:**17b**)
24a	D	5.2	98.0
24b	D	4.7	93.6
8a	C	7.3	97.9
8b	C	6.7	99.7
8c	A	3.5	98.9 (18:1 of **8c**:**8d**)
8d	A	3.8	96.0 (1:4 of **8c**:**8d**)
9a,**b**	A	3.0	95.8 (1:10 of **9a**:**9b**)
29a,**b**	B	3.7	98.1 (1:21 of **29a**:**29b**)
rac-**30**	B	7.6	95.7
31a	B	5.8	97.6
31b	B	6.7	97.3

Na_2SO_4, filtered, concentrated in vacuo, and purified by flash chromatography (petroleum ether/ethyl acetate; 85/15) to give (2*S*)-*N*-(*tert*-butoxycarbonyl)proline methyl ester (0.552 g, 40% yield). ^{1}H NMR ($CDCl_3$, 300 MHz) δ 4.21 (dd, lH), 3 70 (s, 3H), 3.58−3.30 (m, 2H), 2.30−1.75 (m, 4H), 1.40 (s, 9H).

(2*S*)-*N*-(*tert*-Butoxycarbonyl)pyrrolidine-2-carboxamide.[43] (2*S*)-*N*-(*tert*-Butoxycarbonyl)proline methyl ester (0.552 g, 2.4 mmol) was heated in a mixture of THF and 28% aqueous NH_3 (2/9, v/v) at 60 °C for 18 h under Ar. The reaction mixture was concentrated to give Boc-L-Pro-NH_2 (0.460 g, 89%), used in the next step without any further purification. ^{1}H NMR (400 MHz, $CDCl_3$) δ 7.50−7.01 (m, 2H), 4.87 (m, 1H), 4.35 (m, 1H), 3.44 (m, 1H), 2.00−1.75 (m, 4H), 1.43 (s, 9H).

(2*S*)-*N*-(*tert*-Butoxycarbonyl)-pyrrolidine-2-carbonitrile.[43] TFA anhydride (0.39 mL, 2.80 mmol) was added to a solution of (2*S*)-*N*-(*tert*-butoxycarbonyl)pyrrolidine-2-carboxamide (0.501 g, 2.33 mmol) and Et_3N (0.779 mL, 5.59 mmol) in dry THF (6 mL) under Ar at 0 °C. The reaction was stirred at 0 °C for another 6 h. After addition of CH_2Cl_2, the organic phase was washed with a saturated aqueous $NaHCO_3$ solution, dried over Na_2SO_4, filtered, and concentrated in vacuo to afford (2*S*)-*N*-(*tert*-butoxycarbonyl)-pyrrolidine-2-carbonitrile (0.393 g, 86%, brown oil) used in the next step without any further purification. ^{1}H NMR (400 MHz, $CDCl_3$) δ 4.43 (m, 1H), 3.54−3.30 (m, 2H), 2.30−1.98 (m, 4H), 1.49 (s, 9H).

(2*S*)-Pyrrolidine-2-carbonitrile (TFA Salt).[44] (2*S*)-*N*-(*tert*-Butoxycarbonyl)-pyrrolidine-2-carbonitrile (0.202 g, 1.03 mmol) was dissolved in dry CH_2Cl_2 (5 mL) under Ar and TFA (2 mL) was added at 0 °C. The reaction was stirred at 0 °C for 2 h. The solvent was evaporated and the product was crystallized in Et_2O, yielding the white TFA salt of (2*S*)-pyrrolidine-2-carbonitrile (0.110 g, 51% yield, white powder). ^{1}H NMR (400 MHz, CD_3OD) δ 4.92 (s, 1H), 4.68 (t, 1H), 3.47−3.35 (m, 2H), 2.52−2.43 (m, 1H), 2.32−2.07 (m, 3H).

***rac*-*N*-(*tert*-Butoxycarbonyl)-piperidine-2-carboxylic Acid.**[45] DL-Pipecolinic acid (3.00 g, 23.2 mmol) and Et_3N (3.24 mL, 23.2 mmol) were dissolved in 1,4-dioxane (32 mL) and H_2O (21 mL). Boc_2O (5.58 g, 25.5 mmol) was added, and the solution was stirred for 24 h at rt. The solvent was evaporated, and the residue was extracted in EtOAc. The solution was washed with aqueous 5% HCl and brine. The organic layer was dried over Na_2SO_4, filtered, and evaporated to obtain *rac*-*N*-(*tert*-butoxycarbonyl)-piperidine-2-carboxylic acid (4.39 g, 82% yield, white powder). ^{1}H NMR ($CDCl_3$) δ 10.93 (s, 1H), 4.92−4.74 (bd, 1H), 3.98−3.91 (m, 1H), 2.95 (m, 1H), 2.20 (s, 1H), 1.66−1.23 (m, 14H).

***rac*-*N*-(*tert*-Butoxycarbonyl)-piperidine-2-carboxamide.**[43] To a solution of *rac*-*N*-(*tert*-butoxycarbonyl)-piperidine-2-carboxylic acid (4.26 g, 18.6 mmol) and Et_3N (2.60 mL, 18.7 mmol) in dry THF (25 mL) under Ar at −15 °C was added dropwise a solution of ethyl chloroformate. The resulting reaction mixture was stirred for 1 h. Then 28% aqueous NH_3 (6 mL) was then added dropwise and the solution was warmed to rt and stirred for another 4 h. The solution was concentrated and the residue extracted with EtOAc, washed with 10% aqueous citric acid, a saturated aqueous $NaHCO_3$ solution, then brine, dried over Na_2SO_4, filtered, and concentrated in vacuo to give *rac*-*N*-(*tert*-butoxycarbonyl)-piperidine-2-carboxamide (3.53 g, 83% yield, oil). ^{1}H NMR (400 MHz, $CDCl_3$) δ 6.12 (m, 2H), 4.70 (m, 1H), 4.11 (m, 1H), 2.70 (m, 1H), 2.25 (m, 1H), 1.46 (s, 9H), 1.70−1.38 (m, 5H).

***rac*-2-Piperidine-2-carbonitrile (HCl Salt).**[46] A solution of *rac*-*N*-(*tert*-butoxycarbonyl)-piperidine-2-carboxamide (0.100 g, 0.48 mmol) in 1,4-dioxane (5 mL) was treated with 4 N HCl for 45 min at rt. The reaction mixture was then filtered, washed with Et_2O, and concentrated in vacuo to afford the HCL salt of *rac*-2-piperidine-2-carbonitrile (0.064 g, 92% yield, white powder). ^{1}H NMR (400 MHz, CD_3OD) δ 3.84 (d, 1H), 3.38 (d, 1H), 3.03 (t, 1H), 2.24 (d, 1H), 1.94−1.86 (m, 2H), 1.72−1.69 (m, 3H).

General Procedure for Dipeptide Coupling. Anhydrous Et_3N (2 equiv) was added dropwise to a stirred solution of amino acid (1 equiv) (TFA or HCl salt), *N*-benzyloxycarbonyl-glycine or *N*-benzyloxycarbonyl-alanine or *N*-benzyloxycarbonyl-D-alanine (1 equiv) and HOBt (0.6 equiv) in CH_2Cl_2 under Ar. The resulting solution was cooled to 0 °C. A solution of 1-ethyl-3-(3-dimethylaminopropyl)carbodiimide hydrochloride (1.05 equiv) in CH_2Cl_2 was then added dropwise. The reaction mixture was warmed up to rt, stirred until completion (tlc monitoring, 16 to 20 h), and then washed with 0.2 N aqueous HCl, saturated aqueous $NaHCO_3$, dried over Na_2SO_4, filtered, and concentrated in vacuo. Flash chromatography afforded the dipeptides.

***N*-Benzyloxycarbonylamino-glycine-2*S*-pyrrolidine-2-carbonitrile (11a).** Following the general procedure, (2*S*)-pyrrolidine-2-carbonitrile (TFA salt) (0.080 g, 0.38 mmol) reacted with Cbz-Gly-OH afforded after flash chromatography (CH_2Cl_2/acetone; gradient of 98/2 to 95/5) *N*-benzyloxycarbonylamino-glycine-2*S*-pyrrolidine-2-carbonitrile (**11a**) (63 mg, 58%). ^{1}H NMR ($CDCl_3$, 300 MHz) δ 7.41−7.27 (m, 5H), 5.75 (s, 1H), 5.12 (s, 2H), 4.74 (m, 1H), 4.05 (dd, 1H), 3.94 (dd, 1H), 3.59 (m, 1H), 3.41 (m, 1H), 2.35−2.07 (m, 4H). ^{13}C NMR ($CDCl_3$, 75 MHz) δ 167.6, 156.5, 136.4, 128.6, 128.3, 128.1, 118.1, 67.1, 46.7, 45.5, 43.6, 30.0, 25.2. HRMS (ESI+) calcd for $[C_{15}H_{17}N_3O_3 + Na]^+$: 310.11621. Found: 310.11591.

***N*-Benzyloxycarbonylamino-L-alanine-2*S*-pyrrolidine-2-carbonitrile (12a).** Following the general procedure, (2*S*)-pyrrolidine-2-carbonitrile (TFA salt) (0.075 g, 0.36 mmol) reacted with Cbz-L-Ala-OH afforded, after flash chromatography (petroleum ether/ethyl acetate; gradient of 5/2 to 5/3), *N*-benzyloxycarbonylamino-L-alanine-2*S*-pyrrolidine-2-carbonitrile (**12a**) (37 mg, 34%). ^{1}H NMR ($CDCl_3$, 300 MHz) δ 7.39−7.29 (m, 5H), 5.59 (d, 1H), 5.08 (dd, 2H), 4.78 (m, 1H), 4.48 (m, 1H), 3.66 (m, 2H), 2.34−2.11 (m, 3H), 1.65 (m, 1H,), 1.38 (d, 3H). ^{13}C NMR ($CDCl_3$, 75 MHz) δ 171.8, 155.8, 136.4, 128.7, 128.3, 128.1, 118.2, 67.1, 48.4, 46.6, 46.5, 29.9, 25.4, 18.4. HRMS (ESI+) calcd for $[C_{16}H_{19}N_3O_3 + Na]^+$: 324.13186. Found: 324.13168.

***N*-Benzyloxycarbonylamino-D-alanine-2*S*-pyrrolidine-2-carbonitrile (12b).** Following the general procedure, (2*S*)-pyrrolidine-2-carbonitrile (TFA salt) (0.080 g, 0.38 mmol) reacted with Cbz-D-Ala-OH afforded after flash chromatography (hexanes/ethyl acetate; gradient of 5/2 to 6/4) *N*-benzyloxycarbonylamino-D-alanine-2*S*-pyrrolidine-2-carbonitrile (**12b**) (56 mg, 49%). Mixture of rotamers. ^{1}H NMR ($CDCl_3$, 400 MHz) δ 7.41−7.28 (m, 5H), 5.70 (d, 1H), 5.40 (d, 1H), 5.11 (m, 2H), 4.67 (m, 1H), 4.53 (m, 1H), 3.87−3.78 (m, 1H), 3.65−3.42 (m, 1H), 2.42−2.06 (m, 4H), 1.45 (d, 3H), 1.34 (d, 3H). ^{13}C NMR ($CDCl_3$, 75 MHz) δ 171.5; 155.6, 136.3, 128.7, 128.3, 128.1, 118.1, 67.2, 67.1, 48.5,

48.4, 47.4, 46.9, 46.5, 46.4, 32.4, 30.1, 25.2, 23.2, 18.6, 18.2. HRMS (ESI+) calcd for $[C_{16}H_{19}N_3O_3 + Na]^+$: 324.13186. Found: 324.13189.

***N*-Benzyloxycarbonylamino-glycine-2*R*-pyrrolidine-2-carbonitrile (11b).** Following the general procedure, (2*R*)-pyrrolidine-2-carbonitrile (TFA salt) (0.034 g, 0.16 mmol) reacted with Cbz-Gly-OH afforded after flash chromatography (CH_2Cl_2/acetone gradient of 98/2 to 95/5) *N*-benzyloxycarbonylamino-glycine-2*R*-pyrrolidine-2-carbonitrile (**11b**) (31 mg, 66%). ^{1}H NMR ($CDCl_3$, 400 MHz) same as **11a**. ^{13}C NMR ($CDCl_3$, 75 MHz) same as **11a**. HRMS (ESI+) calcd for $[C_{15}H_{17}N_3O_3 + Na]^+$: 310.11621. Found: 310.11621.

***N*-Benzyloxycarbonylamino-glycine-*rac*-piperidine-2-carbonitrile (14).** Following the general procedure, *rac*-2-piperidine-2-carbonitrile (HCl salt) (0.100 g, 0.691 mmol) reacted with Cbz-Gly-OH afforded after flash chromatography (CH_2Cl_2/acetone (gradient of 98/2 to 95/5) *N*-benzyloxycarbonylamino-glycine-*rac*-piperidine-2-carbonitrile (**14**) (31 mg, 30%). ^{1}H NMR ($CDCl_3$, 400 MHz) δ 7.42−7.29 (m, 5H), 5.75 (bs, 1H), 5.68 (bs, 1H), 5.13 (s, 2H), 4.13 (dd, 1H), 3.98 (dd, 1H), 3.70 (m, 1H), 3.31 (m, 1H), 2.08−1.40 (m, 6H). ^{13}C NMR ($CDCl_3$, 125 MHz) δ 167.4, 156.4, 136.4, 128.7, 128.2, 117.1, 67.2, 42.9, 42.4, 41.8, 28.4, 25.1, 20.5. HRMS (ESI+) calcd for $[C_{16}H_{19}N_3O3 + Na]^+$: 324.13186. Found: 324.13187.

General Procedure for the Formation of the Bicyclic Scaffolds. Synthesis of *rac*-16. To a suspension of allylglycine (*rac*-**15**, 550 mg, 4.78 mmol) in 11 mL of dry MeOH at 0 °C was added TMSCl (1.9 mL, 15.0 mmol). The resulting mixture was stirred at 0 °C for 2 h. After stirring for another 12 h at rt, the mixture was cooled to 0 °C and Et_3N (2.70 mL, 19.4 mmol) was slowly added, followed by CBzCl (0.80 mL, 5.68 mmol). The reaction was stirred for 4 h at 0 °C, concentrated in vacuo, dissolved in 2 M HCl, and extracted with EtOAc. The solution was then dried over Na_2SO_4, filtered, concentrated in vacuo, and used without any further purification in the next reaction.

Ozone was bubbled through a solution of the oil in CH_2Cl_2 (50 mL) at −78 °C for 30 min. Excess of ozone was removed by bubbling argon through the solution. Dimethyl sulfide (2 mL, excess) was then added. The resulting mixture was stirred at rt for 16 h, concentrated in vacuo, redissolved in EtOAc, washed with saturated aqueous $NaHCO_3$, dried over Na_2SO_4, filtered, and concentrated to give a colorless oil which was pure enough to be used in the next step without further purification.

General Procedure for Scaffold Synthesis. A solution of L-cysteine methyl ester (or D-cysteine, L-serine methyl ester, L-threonine methyl ester *rac*-homocysteine) hydrochloride (1.2 to 1.7 equiv) and aldehyde (*rac*-**16**) (1.0 equiv) in pyridine was stirred at rt for 15 h under Ar and then at 50 °C for 3 days. The excess pyridine was evaporated. When L-cysteine methyl ester, L-serine methyl ester, and L-threonine methyl ester were used, the residue was redissolved in CH_2Cl_2, washed with 5% aqueous HCl, saturated aqueous $NaHCO_3$, water, and brine, dried over Na_2SO_4, filtered, and concentrated in vacuo. When D-cysteine and *rac*-homocysteine were reacted, the residue was acidified to about pH 2 with 1N aqueous HCl and partitioned between CH_2Cl_2 and water. The organic layer was washed with brine, dried over Na_2SO_4, filtered, and concentrated in vacuo. The residue was redissolved in THF and treated with a 2.0 M (trimethylsilyl)diazomethane ($TMSCH_2N_2$) solution for 16 h. The solution was then stirred with saturated aqueous $NaHCO_3$ and extracted with CH_2Cl_2. The organic phase was dried over Na_2SO_4, filtered, and concentrated in vacuo. All crude residues were purified by flash chromatography (toluene/diethyl ether, gradient of 9:1 to 8:2) to yield the corresponding bicyclic scaffolds.

(2*R*,5*S*,7*S*)-1-Aza-7-benzyloxycarbonylamino-8-oxo-4-thiabicyclo[3.3.0]octane-2-carboxylic Acid Methyl Ester (17a) and (2*R*,5*S*,7*R*)-1-Aza-7-benzyloxycarbonylamino-8-oxo-4-thiabicyclo[3.3.0]octane-2-carboxylic Acid Methyl Ester (17b). Following the general procedure, L-Cys-OMe (1.00 g, 5.84 mmol) and *rac*-**16** (1.10 g, 4.15 mmol) afforded the corresponding bicyclic scaffolds **17a** (434 mg, 30%) and **17b** (265 mg, 18%). **17a**: ^{1}H NMR (300 MHz, $CDCl_3$) δ 7.36 (s, 5H), 5.23 (bd, 1H), 5.19−5.17 (m, 1H), 5.13 (s, 2H), 5.08−5.04 (m, 1H), 4.50−4.42 (q, 1H), 3.78 (s, 3H), 3.53−3.36 (m, 2H), 2.77−2.70 (m, 1H), 2.49−2.39 (m, 1H). ^{13}C NMR (75 MHz, $CDCl_3$) δ 175.0, 170.2, 156.1, 136.1, 128.6, 128.3, 128.3, 67.3, 64.0, 58.6, 53.1, 52.2, 37.1, 30.0. HRMS (EI+) calcd for $[C_{16}H_{18}N_2O_5S]^+$: 350.09364. Found: 350.09310. **17b**: ^{1}H NMR (300 MHz, $CDCl_3$) δ 7.35 (s, 5H), 5.35 (bd, 1H), 5.16−5.14 (m, 2H), 5.12 (s, 2H), 4.67 (q, 1H), 3.77 (s, 3H), 3.37−3.35 (m, 2H), 3.26−3.15 (m, 1H), 2.10−2.00 (m, 1H). ^{13}C NMR (75 MHz, $CDCl_3$) δ 171.3, 169.6, 156.05, 136.1, 128.7, 128.4, 128.2, 67.2, 61.7, 57.8, 54.7, 53.1, 38.5, 35.1. HRMS (EI+) calcd for $[C_{16}H_{18}N_2O_5S]^+$: 350.09364. Found: 350.09268.

(2*S*,5*R*,7*S*)-1-Aza-7-benzyloxycarbonylamino-8-oxo-4-thiabicyclo[3.3.0]octane-2-carboxylic Acid Methyl Ester (17c) and (2*S*,5*R*,7*R*)-1-Aza-7-benzyloxycarbonylamino-8-oxo-4-thiabicyclo[3.3.0]octane-2-carboxylic Acid Methyl Ester (17d). Following the general procedure and treatment with $TMSCH_2N_2$ (5 mL, excess), D-Cys (1.00 g, 6.35 mmol) and *rac*-**16** (1.10 g, 4.15 mmol) afforded the corresponding bicyclic scaffolds **17c** (194 mg, 13%) and **17d** (291 mg, 20%). The characterization data are the same as for **17a** and **17b**.

(2*S*,5*S*,7*S*)-1-Aza-7-benzyloxycarbonylamino-8-oxo-4-oxabicyclo[3.3.0]octane-2-carboxylic Acid Methyl Ester and (18a) and (2*R*,5*S*,7*R*)-1-Aza-7-benzyloxycarbonylamino-8-oxo-4-oxabicyclo[3.3.0]octane-2-carboxylic Acid Methyl Ester (18b). Following the general procedure, L-Ser-OMe (0.250 g, 1.61 mmol) and *rac*-**16** (0.250 g, 0.943 mmol) afforded the corresponding bicyclic scaffolds **18a** and **18b** as an inseparable mixture (154 mg, 49%). ^{1}H NMR (400 MHz, $CDCl_3$) δ 7.35 (s, 5H), 5.30 (bs, 1H), 5.17−5.19 (d, 1H), 5.13 (s, 2H), 5.09−5.07 (d, 1H), 4.49−4.43 (q, 1H) 3.78 (m, 1H), 2.97−2.90 (m, 1H), 2.69−2.64 (m, 1H), 2.52−2.29 (m, 3H), 1.95−1.86 (m, 1H). ^{13}C NMR (125 MHz, $CDCl_3$) δ 177.4, 174.1, 170.4, 170.0, 156.1, 136.2, 128.7, 128.4, 90.8, 89.3, 89.2, 70.0, 67.4, 57.2, 55.2, 54.1, 53.0, 52.9, 52.5, 36.1, 31.1. HRMS (ESI+) calcd for $[C_{16}H_{18}N_2O_6 + Na]^+$: 357.10571. Found: 357.10533.

(2*S*,3*R*,5*S*,7*S*)-1-Aza-7-benzyloxycarbonylamino-8-oxo-4-oxa-6-methylbicyclo[3.3.0]octane-2-carboxylic Acid Methyl Ester and (19a) (2*S*,3*R*,5*S*,7*R*)-1-Aza-7-benzyloxycarbonylamino-8-oxo-4-oxa-6-methylbicyclo[3.3.0]octane-2-carboxylic Acid Methyl Ester (19b). Following the general procedure, L-Thr-OMe (0.680 g, 4.01 mmol) and *rac*-**16** (0.825 g, 3.11 mmol) afforded the corresponding bicyclic scaffolds **19a** and **19b** as an inseparable mixture (380 mg, 35%). ^{1}H NMR (400 MHz, $CDCl_3$) δ 7.33 (s, 8H), 5.60 (bs, 0.5 H), 5.49 (bs, 1H), 5.20−5.19 (bd, 2H), 5.11 (s, 4H), 4.69−4.67 (q, 1H), 4.43−4.42 (q, 0.5 H), 4.26−4.17 (m, 1.5H), 4.11−4.09 (m, 1.5H), 3.76 (d, 6H), 3.08−3.04 (m, 1H), 2.64−2.58 (m, 0.5H), 2.28−2.22 (m, 0.5 H), 1.96−1.89 (m, 2H), 1.49−1.48 (d, 3H), 1.43−1.42 (d, 2H). ^{13}C NMR (100 MHz, $CDCl_3$) δ 177.40, 173.76, 170.19, 169.74, 156.07, 136.14, 128.63, 128.32, 128.25, 128.20, 90.60, 88.79, 79.82, 79.39, 67.28, 67.22, 63.97, 61.59, 54.03, 52.87, 52.45, 35.89, 31.09, 19.85, 19.39. HRMS (ESI+) calcd for $[C_{17}H_{20}N_2O_6 + Na]^+$: 371.12136. Found: 371.12086.

(2*R*,6*R*,8*R*)-1-Aza-8-benzyloxycarbonylamino-9-oxo-5-thiabicyclo[4.3.0]nonane-2-carboxylic Acid Methyl Ester (*rac*-20). Following the general procedure and treatment with $TMSCH_2N_2$ (5 mL, excess), *rac*-homoCys (0.60 g, 3.50 mmol) and *rac*-**16** (0.568 g, 2.14 mmol) afforded the corresponding bicyclic scaffolds *rac*-**20** (250 mg, 32%). ^{1}H NMR (400 MHz, $CDCl_3$) δ 7.36−7.35 (m, 5H), 5.29 (bd, 1H), 5.19, (d, 1H), 5.12 (s, 2H), 5.07 (dd, 1H), 4.46 (q, 1H), 3.78 (s, 3H), 2.96−2.90 (m, 1H), 2.68 (dt, 1H), 2.49 (m, 1H), 2.39−2.30 (m, 2H), 1.95−1.86 (m,1H). ^{13}C NMR (75 MHz, $CDCl_3$) δ 171.5, 170.3, 156.3, 136.2, 128.7, 128.4, 128.3, 67.3, 54.9, 52.9, 51.9, 51.4, 33.2, 26.8, 25.4. HRMS (ESI+) calcd for $[C_{17}H_{20}N_2O_5S + H]^+$: 365.11657. Found: 365.11685.

(*S*)-Benzyl 5-Oxo-4-(3-oxopropyl)oxazolidine-3-carboxylate (22a) and (*R*)-Benzyl 5-Oxo-4-(3-oxopropyl)oxazolidine-3-carboxylate (22b). To a solution of L- or D-glutamic acid (5.0 g, 34.0 mmol) in 4 N NaOH (17 mL) at 0 °C was added benzyl chloroformate (7.8 mL, 54.7 mmol) dropwise over a period of 10 min and then stirred at rt for 16 h. The solution was extracted with diethyl ether, acidified to pH 2 with 4N HCl, and extracted with ethyl acetate. The organic phase was then dried over Na_2SO_4, filtered, and concentrated in vacuo (5.6 g, 59%, oil). ^{1}H NMR (300 MHz, acetone-d_6) δ 7.29−7.41 (m, 5H), 6.64−6.66 (d, 1H), 5.09 (s, 2H), 4.29−4.36 (m, 1H), 2.47−2.53 (m, 2H), 2.17−2.28 (m, 1H), 1.98−2.05 (m, 1H). To a solution of the crude oil (5.6 g, 20.1 mmol) in toluene (125 mL), under Ar, was added paraformaldehyde (4.02 g, excess) and *p*-toluenesulfonic acid (0.40 g, 2.12 mmol equiv). The mixture was refluxed for 3 h with removal of water using a Dean−Stark and then filtered through a pad of silica and concentrated in vacuo. The crude product was purified by flash chromatography (Hex/EtOAc/AcOH, gradient of 8/2/0.01 to 1/1/0.01) to yield the desired intermediate oxazolidinone (3.02 g, 51%, oil). ^{1}H NMR (400 MHz, $CDCl_3$) δ 7.39−7.35 (m, 5H), 5.55 (br, 1H), 5.24−5.19 (m, 3H), 4.42−4.39 (t, 1H), 2.57−2.15 (m, 4H). To a stirred solution of the intermediate oxazolidinone (2.08 g, 7.1 mmol) in CH_2Cl_2 (50 mL) under Ar were added distilled oxalyl chloride (0.91 mL, 10.6 mmol) and dimethylformamide (0.055 mL, 0.70 mmol). The solution was stirred for 1 h at rt and then the solvents were evaporated to give the crude product (quant. yield), which was immediately dissolved in dry THF (50 mL) and cooled to −78 °C. To the stirred solution was added lithium tri-*tert*-butoxyaluminum hydride (1.89 g, 7.45 mmol) slowly. The mixture was stirred for 4 h, slowly warming to 0 °C, quenched with water, and then filtered through celite. The filtrate was extracted with CH_2Cl_2, washed with water and brine, dried over Na_2SO_4, and concentrated in vacuo to afford the aldehyde **22a** or **22b**, which were used without further purification (1.27 g, 65%, orange oil). ^{1}H NMR (400 MHz, $CDCl_3$) δ 9.70 (br, 1H), 7.41−7.33 (m, 5H), 5.53 (br, 1H), 5.24−5.15 (m, 3H), 4.39−4.36 (t, 1H), 2.70−2.15 (m, 4H).

(2*R*,5*S*,8*S*)-1-Aza-8-benzyloxycarbonylamino-9-oxo-4-thiabicyclo[3.4.0]nonane-2-carboxylic Acid Methyl Ester 23a. Following the general procedure, L-Cys-OMe (0.45 g, 2.6 mmol) and **22a** (0.60 g, 2.16 mmol) provided the cyclized intermediate as an oil. To a solution of this crude mixture in MeOH (25 mL) was added K_2CO_3 (0.40 g, 2.9 mmol). After stirring for another 4 h, the reaction was quenched with water and extracted with CH_2Cl_2. The organic phase was washed with brine, dried over Na_2SO_4, filtered, and concentrated in vacuo. The crude product was purified by flash chromatography (Hex/EtOAc, gradient 6/4 to 1/1) to afford the corresponding bicyclic scaffolds **23a** (116 mg, 32%). ^{1}H NMR (300 MHz, $CDCl_3$) δ 7.36−7.31 (m, 5H), 5.51 (br, 1H), 5.13−5.08 (m, 3H), 4.97−4.90 (m, 1H), 4.33−4.16 (m, 1H), 3.76 (s, 3H), 3.41−3.33 (m, 1H), 3.28−3.21 (m, 1H), 2.65−2.53 (m, 1H), 2.43−1.74 (m, 4H). HRMS (EI+) calcd for $[C_{17}H_{20}N_2O_5S]^+$: 364.10929. Found: 364.10896.

(2*R*,5*S*,8*R*)-1-Aza-8-benzyloxycarbonylamino-9-oxo-4-thiabicyclo[3.4.0]nonane-2-carboxylic Acid Methyl Ester 23b. As for **23a**, L-Cys-OMe (0.95 g, 5.5 mmol), **22b** (1.27 g, 4.60 mmol), and then K_2CO_3 (0.72 g, 5.2 mmol) afforded after flash chromatography (Hex/EtOAc, gradient 6/4 to 1/1) the corresponding bicyclic scaffolds **23b** (372 mg, 25%). HRMS (EI+) calcd for $[C_{17}H_{20}N_2O_5S]^+$: 364.10929. Found: 364.10847.

General Procedure for Formation of the Amides. A stirred solution of the ester (either **24a**−**d**, **25a**,**b**, **26a**,**b**, *rac*-**27**, **28a**,**b**) in a solution of ammonia in methanol (ca. 7N solution) was reacted for 1 h at rt. The corresponding amides were obtained in quantitative yields. Storage leads to partial isomerization. **24a**,**d**, **24b**,**c**, **28a**, and **28b** were fully characterized. However, the other amides (**25a**,**b**, **26a**,**b**, *rac*-**27**) were reacted in the next step without further purification.

(2*R*,5*S*,7*S*)-1-Aza-7-benzyloxycarbonylamino-8-oxo-4-thiabicyclo[3.3.0]octane-2-carboxamide(24a,d). ^{1}H NMR (400 MHz, $(CD_3)_2CO$) δ 7.38−7.36 (m, 5H), 7.11 (bd, 2H), 6.76 (bs, 1H), 5.24−5.23 (dd, 1H), 5.10 (s, 2H), 4.81 (t, 1H), 4.37−4.29 (q, 1H), 3.48−3.47 (m, 2H), 2.58−2.52 (m, 2H). ^{13}C NMR (300 MHz, $(CD_3)_2CO$) δ 174.9, 171.9, 156.8, 137.8, 129.2, 128.8, 128.7, 67.0, 64.9, 60.0, 53.4, 37.0, 31.5. LRMS (ESI+) calcd for $[C_{15}H_{17}N_3O_4S + Na]^+$: 358.08. Found: 358.17.

(2*R*,5*S*,7*R*)-1-Aza-7-benzyloxycarbonylamino-8-oxo-4-thiabicyclo[3.3.0]octane-2-carboxamide (24b,c). ^{1}H NMR (400 MHz, $(CD_3)_2CO$) δ 7.44−7.26 (m, 5H), 7.22 (bs, 1H), 6.75−6.72 (d, 1H), 6.64 (bs, 1H), 5.16 (t, 1H), 5.10 (s, 2H), 4.91−4.89 (m, 1H), 4.84−4.77 (m (1H), 3.52−3.48 (dd, 1H), 3.91−3.24 (m, 1H), 3.07−3.01 (m, 1H), 2.14−2.05 (m, 1H). ^{13}C NMR (75 MHz, $CDCl_3$) δ 172.4, 171.4, 156.9, 138.0, 129.2, 128.7, 66.8, 62.0, 60.3, 55.2, 38.2, 34.8. LRMS (ESI+) calcd for $[C_{15}H_{17}N_3O_4S + Na]^+$: 358.08. Found: 358.15.

(2*R*,5*S*,8*S*)-1-Aza-8-benzyloxycarbonylamino-9-oxo-4-thiabicyclo[3.4.0]nonane-2-carboxamide (28a). ^{1}H NMR (300 MHz, $CDCl_3$) δ 7.41−7.28 (m, 5H), 7.10 (bs, 1H), 5.79 (d, 1H), 5.33−5.28 (m, 2H), 5.08−5.02 (m, 2H), 4.88 (dd, 1H), 3.69 (dd, 1H), 3.53 (dd, 1H), 3.26 (dd, 1H), 2.34 (ddd, 1H), 2.23 (dt, 2H), 1.79 (ddd, 1H). ^{13}C NMR (75 MHz, $CDCl_3$) δ 171.4, 167.7, 156.7, 135.9, 128.7, 128.5, 128.1, 67.5, 62.1, 61.9, 52.1, 30.8, 28.6, 27.4. HRMS (EI+) calcd for $[C_{16}H_{19}N_3O_4S]^+$: 349.10963. Found: 349.10893.

(2*R*,5*S*,8*R*)-1-Aza-8-benzyloxycarbonylamino-9-oxo-4-thiabicyclo[3.4.0]nonane-2-carboxamide (28b). ^{1}H NMR (400 MHz, $CDCl_3$) δ 7.40−7.30 (m, 4H), 6.45 (s, 1H), 5.63 (s, 1H), 5.35 (s, 1H), 5.21−5.15 (m, 1H), 5.13 (s, 2H), 4.86 (t, 1H), 4.34−4.20 (m, 1H), 3.67 (dd, 1H), 3.12 (dd, 1H), 2.48−2.38 (m, 1H), 2.38−2.25 (m, 1H), 2.13−2.02 (m, 1H), 1.87−1.74 (m, 1H). ^{13}C NMR (75 MHz, $CDCl_3$) δ 171.0, 169.8, 156.3, 136.3, 128.7, 128.4, 128.3, 67.2, 61.8, 61.1, 51.6, 30.2, 29.8, 25.3, 24.9. HRMS (EI+) calcd for $[C_{16}H_{19}N_3O_4S]^+$: 349.10963. Found: 349.10863.

General Procedure for Formation of the Nitriles. To a stirred solution of the amide (either **24a**,**d**, **24b**,**c**, **25a**,**b**, **26a**,**b**, *rac*-**27**, **28a**, or **28b**) in dry THF, under Ar, at 0 °C, was added TFA anhydride (1.2 equiv) and Et_3N (2.0 equiv). The reaction was stirred for 1 to 3 h at rt. The solution was extracted with CH_2Cl_2, washed with a saturated $NaHCO_3$, dried over Na_2SO_4, and concentrated in vacuo. Further purification of the residue by flash column chromatography afforded the nitrile derivative.

(2*R*,5*S*,7*S*)-1-Aza-7-benzyloxycarbonylamino-8-oxo-4-thiabicyclo[3.3.0]octane-2-carbonitrile (8a) and (2*S*,5*R*,7*R*)-1-Aza-7-benzyloxycarbonylamino-8-oxo-4-thiabicyclo[3.3.0]octane-2-carbonitrile (8d). Following the general procedure for formation of the nitrile, **24a** (238 mg, 0.71 mmol) or **24d** (90 mg, 0.12 mmol) afforded **8a** (114 mg, 51%) or **8d** (69 mg, 81%). ^{1}H NMR (400 MHz, $(CD_3)_2CO$) δ 7.42−7.29 (m, 5H), 7.07 (d, 1H), 5.42−5.41 (m, 1H), 5.40 (d, 1H), 5.10 (s, 2H), 4.39 (q, 1H), 3.74−3.68 (m, 1H), 3.52−3.48 (m, 1H), 2.71−2.55 (m, 2H). ^{13}C NMR (75 MHz, $(CD_3)_2CO$) δ 175.6, 156.8, 137.9, 129.2, 128.8, 118.1, 67.1, 64.5, 52.2, 48.3, 39.0. HRMS (ESI+) calcd for $[C_{15}H_{15}N_3O_3S + Na]^+$: 340.07263. Found: 340.07229.

(2*R*,5*S*,7*R*)-1-Aza-7-benzyloxycarbonylamino-8-oxo-4-thiabicyclo[3.3.0]octane-2-carbonitrile (8b) and (2*S*,5*R*,7*S*)-1-Aza-7-benzyloxycarbonylamino-8-oxo-4-thiabicyclo[3.3.0]octane-2-carbonitrile (8c). Following the general procedure for formation of the nitrile, **24b** (15 mg, 0.04 mmol) or **24c** (55 mg, 0.16 mmol) afforded **8b** (11 mg, 79%) or **8c** (40 mg, 77%). ^{1}H NMR (400 MHz, $(CD_3)_2CO$) δ 7.38−7.25 (m, 5H), 6.80 (d, 1H), 5.55−5.51 (m, 1H), 5.75 (t, 1H), 5.08 (s, 2H), 4.79−4.72 (m, 1H), 3.49−3.37 (m, 2H), 3.14−3.07 (m, 1H), 2.26−2.18 (m, 1H). ^{13}C NMR (75 MHz, $(CD_3)_2CO$) δ 172.4, 156.7, 138.0, 129.2, 128.7, 128.7, 117.5, 114.0, 66.9, 61.6, 55.0, 54.8, 48.1, 37.8, 36.6. HRMS (ESI+) calcd for $[C_{15}H_{15}N_3O_3S + Na]^+$: 340.07263. Found: 340.07247.

(2S,5*S*,7*S*)-1-Aza-7-benzyloxycarbonylamino-8-oxo-4-oxabicyclo[3.3.0]octane-2-carbonitrile and (9a) (2*R*,5*S*,7*R*)-1-Aza-7-benzyloxycarbonylamino-8-oxo-4-oxabicyclo[3.3.0]octane-2-carbonitrile (9b). Following the general procedure for formation of the nitrile, **25a**,**b** (17 mg, 0.05 mmol) afforded **9a**,**b** (10 mg, 66%). ^{1}H NMR (400 MHz, $CDCl_3$) δ 7.36 (s, 6H), 5.13−5.30 (m, 3H), 5.12 (s, 3H), 4.77−4.84 (m, 1H), 4.59−4.65 (m, 1H), 4.47−4.52 (m, 1H), 4.38−4.43 (m 0.3H), 4.02−4.24 (m, 1.7H), 3.72−3.78 (m, 0.3H), 3.09−3.16 (m, 1H), 2.67−2.74 (m, 0.3H), 2.36−2.44 (m, 0.3H), 2.01−2.08 (m, 1H). ^{13}C NMR (125 MHz, $CDCl_3$) δ 174.4, 155.9, 135.9, 128.7, 128.5, 128.4, 128.3, 116.8, 116.4, 90.6, 89.1, 70.7, 70.6, 67.5, 53.7, 45.4, 43.4, 35.1. HRMS (ESI+) calcd for $[C_{15}H_{15}N_3O_4 + Na]^+$: 324.09548. Found: 324.09527.

(2S,3*R*,5*S*,7*S*)-1-Aza-7-benzyloxycarbonylamino-8-oxo-4-oxa-6-methylbicyclo[3.3.0]octane-2-carbonitrile and (29a) (2S,3*R*,5*S*,7*R*)-1-Aza-7-benzyloxycarbonylamino-8-oxo-4-oxa-6-methylbicyclo[3.3.0]octane-2-carbonitrile (29b). Following the general procedure for formation of the nitrile, **26a**,**b** (100 mg, 0.30 mmol) afforded **29a**,**b** (51 mg, 54%). ^{1}H NMR (400 MHz, $CDCl_3$) δ 7.36 (s, 5H), 5.30−5.23 (m, 2H), 5.12 (s, 2H), 4.63 (q, 1H), 4.43 (q, 1H), 4.20 (q, 1H), 3.17−3.09 (m, 1H), 2.71−2.64 (m, 0.1H), 2.41−2.33 (m, 0.1H), 2.05−1.97 (m, 1H), 1.53−1.51 (d, 3H), 1.43 (d, 1H). ^{13}C NMR (75 MHz, $CDCl_3$) δ 174.4, 155.9, 136.0, 128.7, 128.5, 128.3, 116.5, 116.1, 90.5, 88.9, 80.7, 67.5, 53.5, 51.9, 49.4, 35.3, 18.9, 18.2. HRMS (ESI+) calcd for $[C_{16}H_{17}N_3O_4 + Na]^+$: 338.11113. Found: 338.11096.

(2*RS*,6*RS*,8*RS*)-1-Aza-8-benzyloxycarbonylamino-9-oxo-5-thiabicyclo[4.3.0]nonane-2-carbonitrile (*rac*-30). Following the general procedure for formation of the nitrile, *rac*-**27** (59 mg, 0.17 mmol) afforded *rac*-**30** (24 mg, 42%). ^{1}H NMR (400 MHz, $CDCl_3$) δ 7.36 (s, 5H), 5.42 (bs, 1H), 5.20 (bs, 2H), 5.13 (s, 2H), 4.42 (q, 1H), 3.35 (t, 1H), 2.83−2.79 (m, 1H), 2.53−2.48 (m, 1H), 2.41−2.33 (m, 1H), 2.33−2.17 (m, 1H), 2.00−1.94 (m, 1H). ^{13}C NMR (100 MHz, $CDCl_3$) δ 170.5, 156.1, 136.0, 128.7, 128.5, 128.3, 115.9, 67.5, 54.4, 51.4, 41.9, 32.8, 28.2, 24.8. HRMS (ESI+) calcd for $[C_{16}H_{17}N_3O_3S + Na]^+$: 354.08828. Found: 354.08831.

(2*R*,5*S*,8*S*)-1-Aza-8-benzyloxycarbonylamino-9-oxo-4-thiabicyclo[3.4.0]nonane-2-carboxylic Carbonitrile (31a). Following the general procedure for formation of the nitrile, **28a** (23 mg, 0.07 mmol) afforded **31a** (9 mg, 39%). ^{1}H NMR (500 MHz, $CDCl_3$) δ 7.42−7.28 (m, 5H), 5.62 (s, 1H), 5.34 (dd, 1H), 5.12 (q, 2H), 4.95 (s, 1H), 4.23 (s, 1H), 3.40 (dd, 1H), 3.31 (dd, 1H), 2.53 (bd, 1H), 2.40 (bd, 1H), 1.97−1.78 (m, 2H). ^{13}C NMR (125 MHz, $CDCl_3$) δ 167.6, 156.6, 136.3, 128.7, 128.7, 128.6, 128.3, 128.2, 116.7, 67.2, 62.3, 52.3, 48.5, 33.2, 29.8, 27.9, 27.7. HRMS (EI+) calcd for $[C_{16}H_{17}N_3O_3S]^+$: 331.09906. Found: 331.09817.

(2*R*,5*S*,8*R*)-1-Aza-8-benzyloxycarbonylamino-9-oxo-4-thiabicyclo[3.4.0]nonane-2-carboxylic Carbonitrile (31b). Following the general procedure for formation of the nitrile, **28b** (40 mg, 0.11 mmol) afforded **31b** (10 mg, 27%). ^{1}H NMR (500 MHz, $CDCl_3$) δ 7.36 (s, 5H), 5.74 (s, 1H), 5.68 (s, 1H), 5.12 (s, 3H), 4.30−4.18 (m, 1H), 3.30 (dd, 2H), 2.52−2.31 (m, 2H), 2.19−2.02 (m, 1H), 1.92−1.76 (m, 1H). ^{13}C NMR (125 MHz, CDCl3) δ 168.7, 156.1, 136.2, 128.7, 128.4, 128.3, 116.8, 67.2, 61.9, 51.8, 48.5, 33.7, 29.8, 24.9. HRMS (EI+) calcd for $[C_{17}H_{20}N_2O_5S]^+$: 331.09906. Found: 331.09795.

HPLC Analysis of Purity. To verify the purity of all compounds used for biological tests, analytical reverse phase HPLC was performed on an Agilent 1100 series instrument equipped with VWD-detector, C18 reverse column (Agilent, Zorbax Eclipse XDB-C18 150 mm × 4.6 mm, 5 μm), UV detection at 254 nm. Depending on the compound, two different conditions were used: condition A (50% acetonitrile, 50% water, 1 mL/min), condition B (50% methanol, 50% water, 1 mL/min), condition C (60% water, 40% acetonitrile, 1 mL/min), or condition D (70% water, 30% acetonitrile, 1 mL/min) (Table 4).

Docking Study. The protein structure (1H2Y) was downloaded from the Protein Data Bank and prepared as reported previously.[19] It was next prepared for docking using PROCESS, a module of our docking program FITTED.[21] The ligands were prepared using Maestro and SMART, a third module of FITTED. They were subsequently docked using the FITTED docking engine and defaults parameters. For the covalent docking to be used, the Ser554 has been selected as a reactive residue.

Biological Evaluations. The human glioblastoma-derived cell lines LN18, LN229, and LNZ308 were a kind gift of AC Diserens, Neurosurgery Department, Lausanne, Switzerland, the immortalized human brain-derived HCEC cells have been kindly provided by D. Stanimirovic, Ottawa, Canada, and the human fibroblasts PO03 and PG98/5 cells have been prepared in Lausanne from human lung and skin surgical samples, respectively, according to protocols accepted by the Hospital Ethics Committee.

Cells were routinely grown in DMEM culture medium containing 4.5 gL glucose, 10% fetal calf serum (FCS), and antibiotics (all from Gibco, Basel, Switzerland). One to two days before evaluation, cells were seeded in 48-well plates (Costar, Corning, NY) in complete medium in order to reach confluence on the day of experiment. On the day of experiment, the culture medium was removed, and either 200 μL phosphate-buffered saline (PBS, pH 7.2−7.4) was added in half of the wells or 200 μL PBS containing 0.1% Triton X-100 (Fluka, Buchs, Switzerland) was added in the other half of the wells, for the evaluation of the inhibition of POP and DPP IV activities in intact cells or cell extracts, respectively. Experiments were performed in duplicate wells.

The synthetic molecules were dissolved at 10 mg/mL in methanol and then diluted 1:10 in H_2O, and 1 or 5 μL of the water solution were added to duplicate PBS and PBS-Triton wells, followed after 5−10 min at room temperature by 1 μL of Gly-Pro-AMC or Z-Gly-Pro-AMC substrates (1 mg/mL DMSO, both from Bachem, Bubendorf, Switzerland), final concentration 10 μM. Increase in fluorescence at $\lambda_{ex}/\lambda_{em}$ = 360/460 nm was recorded for 30 min at 37 °C in a thermostatted multiwell fluorescence reader (Cytofluor, PerSeptive BioSystems, Switzerland). For the determination of IC_{50}, cells in PBS or in PBS-Triton X-100 were exposed to decreasing concentrations of the inhibitors and then determination of residual activity was measured and plotted against inhibitor concentration. IC_{50} values were determined graphically.

Acknowledgment. We thank CIHR, ViroChem Pharma, NSERC, FQRNT, and the Canadian Foundation for Innovation for financial support (N.M.). J.L. holds a scholarship from Le Fonds Québécois de la Recherche sur la Nature et les Technologies. We also thank the Swiss Society for Multiple Sclerosis for support to L.J-J.'s group.

References

(1) Polgar, L. Unusual secondary specificity of prolyl oligopeptidase and the different reactivities of its two forms toward charged substrates. *Biochemistry* **1992**, *31*, 7729–7735.
(2) Irazusta, J.; Larrinaga, G.; Gonzalez-Maeso, J.; Gil, J.; Meana, J. J.; Casis, L. Distribution of prolyl endopeptidase activities in rat and human brain. *Neurochem. Int.* **2002**, *40*, 337–345.
(3) Szeltner, Z.; Polgar, L. Structure, function and biological relevance of prolyl oligopeptidase. *Curr. Prot. Pept. Sci.* **2008**, *9*, 96–107.
(4) Männisto, P. T.; Vanäläinen, J.; Jalkanen, A.; Garcia-Horsman, J. A. Prolyl oligopeptidase: A potential target for the treatment of cognitive disorders. *Drug News Perspect.* **2007**, *20*, 293–305.
(5) Brandt, I.; Scharpe, S.; Lambeir, A. M. Suggested functions for prolyl oligopeptidase: A puzzling paradox. *Clin. Chim. Acta* **2007**, *377*, 50–61.
(6) Williams, R. S. B. Prolyl oligopeptidase and bipolar disorder. *Clin. Neurosci. Res.* **2004**, *4*, 233–242.
(7) Cunningham, D. F.; O'Connor, B. Identification and initial characterisation of a *N*-benzyloxycarbonyl-prolyl-prolinal (*Z*-Pro-prolinal)-insensitive 7-(*N*-benzyloxycarbonyl-glycyl-prolyl-amido)-4- methylcoumarin (*Z*-Gly-Bro-NH-Mec)-hydrolysing peptidase in bovine serum. *Eur. J. Biochem.* **1997**, *244*, 900–903.
(8) Toide, K.; Shinoda, M.; Iwamoto, Y.; Fujiwara, T.; Okamiya, K.; Uemura, A. A novel propyl endopeptidase inhibitor, JTP-4819, with potential for treating Alzheimer's disease. *Behav. Brain Res.* **1997**, *83*, 147–151.

(9) Toide, K.; Shinoda, M.; Miyazaki, A. A novel prolyl endopeptidase inhibitor, JTP-4819. Its behavioral and neurochemical properties for the treatment of Alzheimer's disease. *Rev. Neurosci.* **1998**, *9*, 17–29.
(10) Saito, M.; Hashimoto, M.; Kawaguchi, N.; Shibata, H.; Fukami, H.; Tanaka, T.; Higuchi, N. Synthesis and inhibitory activity of acyl-peptidyl-pyrrolidine derivatives toward post-proline cleaving enzyme; a study of subsite specificity. *J. Enzyme Inhib.* **1991**, *5*, 51–75.
(11) Barelli, H.; Petit, A.; Hirsch, E.; Wilk, S.; De Nanteuil, G.; Morain, P.; Checler, F. S 17092-1, a highly potent, specific and cell permeant inhibitor of human proline endopeptidase. *Biochem. Biophys. Res. Commun.* **1999**, *257*, 657–661.
(12) Toide, K.; Shinoda, M.; Fujiwara, T.; Iwamoto, Y. Effect of a novel prolyl endopeptidase inhibitor, JTP-4819, on spatial memory and central cholinergic neurons in aged rats. *Pharmacol., Biochem. Behav.* **1997**, *56*, 427–434.
(13) Miyazaki, A.; Toide, K.; Sasaki, Y.; Ichitani, Y.; Iwasaki, T. Effect of a prolyl endopeptidase inhibitor, JTP-4819, on radial maze performance in hippocampal-lesioned rats. *Pharmacol., Biochem. Behav.* **1998**, *59*, 361–368.
(14) Kato, A.; Fukunari, A.; Sakai, Y.; Nakajima, T. Prevention of amyloid-like deposition by a selective prolyl endopeptidase inhibitor, Y-29794, in senescence-accelerated mouse. *J. Pharmacol. Exp. Ther.* **1997**, *283*, 328–335.
(15) Shinoda, M.; Toide, K.; Ohsawa, I.; Kohsaka, S. Specific inhibitor for prolyl endopeptidase suppresses the generation of amyloid β protein in NG108-15 cells. *Biochem. Biophys. Res. Commun.* **1997**, *235*, 641–645.
(16) Morain, P.; Robin, J. L.; De Nanteuil, G.; Jochemsen, R.; Heidet, V.; Guez, D. Pharmacodynamic and pharmacokinetic profile of S 17092, a new orally active prolyl endopeptidase inhibitor, in elderly healthy volunteers. A phase I study. *Br. J. Clin. Pharmacol.* **2000**, *50*, 350–359.
(17) Szeltner, Z.; Rea, D.; Renner, V.; Fülöp, V.; Polgár, L. Electrostatic effects and binding determinants in the catalysis of prolyl oligopeptidase: Site-specific mutagenesis at the oxyanion binding site. *J. Biol. Chem.* **2002**, *277*, 42613–42622.
(18) Li, J.; Wilk, E.; Wilk, S. Inhibition of prolyl oligopeptidase by Fmoc-aminoacylpyrrolidine-2-nitriles. *J. Neurochem.* **1996**, *66*, 2105–2112.
(19) Corbeil, C. R.; Englebienne, P.; Moitessier, N. Docking Ligands into Flexible and Solvated Macromolecules. 1. Development and Validation of FITTED 1.0. *J. Chem. Inf. Model.* **2007**, *47*, 435–449.
(20) Corbeil, C. R.; Moitessier, N. Docking Ligands into Flexible and Solvated Macromolecules. 3. Impact of Input Ligand Conformation, Protein Flexibility and Water Molecules on the Accuracy of Docking Programs. *J. Chem. Inf. Model.* **2009**, *49*, 997–1009.
(21) Corbeil, C. R.; Englebienne, P.; Moitessier, N.; Therrien, E. *FITTED Docking Program*; www.fitted.ca **2009**.
(22) Oballa, R. M.; Truchon, J. F.; Bayly, C. I.; Chauret, N.; Day, S.; Crane, S.; Berthelette, C. A generally applicable method for assessing the electrophilicity and reactivity of diverse nitrile-containing compounds. *Bioorg. Med. Chem. Lett.* **2007**, *17*, 998–1002.
(23) Hanessian, S.; Moitessier, N. Sulfonamide-based acyclic and conformationally constrained MMP inhibitors: from computer-assisted design to nanomolar compounds. *Curr. Top. Med. Chem.* **2004**, *4*, 1269–1287.
(24) Hanessian, S.; McNaughton-Smith, G.; Lombart, H.-G.; Lubell, W. D. Design and synthesis of conformationally constrained amino acids as versatile scaffolds and peptide mimetics. *Tetrahedron* **1997**, *53*, 12789–12854.
(25) Baldwin, J. E.; Freeman, R. T.; Lowe, C.; Schofield, C. J.; Lee, E. A [gamma]-lactam analogue of the penems possessing antibacterial activity. *Tetrahedron* **1989**, *45*, 4537–4550.
(26) Subasinghe, N. L.; Bontems, R. J.; McIntee, E.; Mishra, R. K.; Johnson, R. L. Bicyclic thiazolidine lactam peptidomimetics of the dopamine receptor modulating peptide Pro-Leu-Gly-NH_2. *J. Med. Chem.* **1993**, *36*, 2356–2361.
(27) Nagai, U.; Sato, K. Synthesis of a bicyclic dipeptide with the shape of [beta]-turn central part. *Tetrahedron Lett.* **1985**, *26*, 647–650.
(28) Estiarte, M. A.; Rubiralta, M.; Diez, A.; Thormann, M.; Giralt, E. Oxazolopiperidin-2-ones as Type II' beta-Turn Mimetics: Synthesis and Conformational Analysis. *J. Org. Chem.* **2000**, *65*, 6992–6999.
(29) Caplan, J. F.; Sutherland, A.; Vederas, J. C. The first stereospecific synthesis of L-tetrahydrodipicolinic acid: a key intermediate of diaminopimelate metabolism. *J. Chem. Soc., Perkin Trans. 1* **2001**, 2217–2220.
(30) Kamber, M.; Just, G. gamma-Phosphono-gamma-lactones. The use of allyl esters as easily removable phosphonate protecting groups. *Can. J. Chem.* **1985**, *63*, 823–827.
(31) Khalil, E. M.; Pradhan, A.; Ojala, W. H.; Gleason, W. B.; Mishra, R. K.; Johnson, R. L. Synthesis and Dopamine Receptor Modulating Activity of Substituted Bicyclic Thiazolidine Lactam Peptidomimetics of l-Prolyl-l-leucyl-glycinamide. *J. Med. Chem.* **1999**, *42*, 2977–2987.
(32) Wallen, E. A. A.; Christiaans, J. A. M.; Forsberg, M. M.; Venalainen, J. I.; Mannisto, P. T.; Gynther, J. Dicarboxylic acid bis(L-prolyl-pyrrolidine) amides as prolyl oligopeptidase inhibitors. *J. Med. Chem.* **2002**, *45*, 4581–4584.
(33) Baldwin, J. E.; Lee, E. Synthesis of bicyclic γ-lactams via oxazolidinones. *Tetrahedron* **1986**, *42*, 6551–6554.
(34) Juillerat-Jeanneret, L. Prolyl-specific peptidases and their inhibitors in biological processes. *Curr. Chem. Biol.* **2008**, *2*, 97–109.
(35) Morain, P.; Lestage, P.; De Nanteuil, G.; Jochemsen, R.; Robin, J. L.; Guez, D.; Boyer, P. A. S 17092: a prolyl endopeptidase inhibitor as a potential therapeutic drug for memory impairment. Preclinical and clinical studies. *CNS Drug Rev.* **2002**, *8*, 31–52.
(36) Toide, K.; Iwamoto, Y.; Fujiwara, T.; Abe, H. JTP-4819: A novel prolyl endopeptidase inhibitor with potential as a cognitive enhancer. *J. Pharmacol. Exp. Ther.* **1995**, *274*, 1370–1378.
(37) Schneider, J. S.; Giardiniere, M.; Morain, P. Effects of the prolyl endopeptidase inhibitor S 17092 on cognitive deficits in chronic low dose MPTP-treated monkeys. *Neuropsychopharmacology* **2002**, *26*, 176–182.
(38) Maes, M. Alterations in plasma prolyl endopeptidase activity in depression, mania, and schizophrenia: effects of antidepressants, mood stabilizers, and antipsychotic drugs. *Psychiatry Res.* **1995**, *58*, 217–225.
(39) Mantle, D.; Falkous, G.; Ishiura, S.; Blanchard, P. J.; Perry, E. K. Comparison of proline endopeptidase activity in brain tissue from normal cases and cases with Alzheimer's disease, Lewy body dementia, Parkinson's disease and Huntington's disease. *Clin. Chim. Acta* **1996**, *249*, 129–139.
(40) Tran, T.; Quan, C.; Edosada, C. Y.; Mayeda, M.; Wiesmann, C.; Sutherlin, D.; Wolf, B. B. Synthesis and structure−activity relationship of *N*-acyl-Gly−, *N*-acyl-Sar−, and *N*-blocked-boroPro inhibitors of FAP, DPP4, and POP. *Bioorg. Med. Chem. Lett.* **2007**, *17*, 1438–1442.
(41) Yoshimoto, T.; Tsuru, D.; Yamamoto, N.; Ikezawa, R.; Furukawa, S. Structure−Activity Relationship of Inhibitors Specific for Prolyl Endopeptidase. *Agric. Biol. Chem.* **1991**, *55*, 37–43.
(42) Jones, K.; Woo, K.-C. A total synthesis of (−)-ruspolinone. *Tetrahedron* **1991**, *47*, 7179–7184.
(43) Tang, F. Y.; Qu, L. Q.; Xu, Y.; Ma, R. J.; Chen, S.-H.; Li, G. Practical Synthesis of Structurally Important Spirodiamine Templates. *Synth. Commun.* **2007**, *37*, 3793–3799.
(44) Caputo, C. A.; Carneiro, F. d. S.; Jennings, M. C.; Jones, N. D. Modular syntheses of oxazolinylamine ligands and characterization of group 10 metal complexes. *Can. J. Chem.* **2007**, *85*, 85–95.
(45) Heller, B.; Sundermann, B.; Buschmann, H.; Drexler, H. J.; You, J.; Holzgrabe, U.; Heller, E.; Oehme, G. Photocatalyzed [2 + 2 + 2]-Cycloaddition of Nitriles with Acetylene: An Effective Method for the Synthesis of 2-Pyridines under Mild Conditions. *J. Org. Chem.* **2002**, *67*, 4414–4422.
(46) Johnson, R. L.; Rajakumar, G.; Yu, K. L.; Mishra, R. K. Synthesis of Pro-Leu-Gly-NH_2 analogs modified at the prolyl residue and evaluation of their effects on the receptor binding activity of the central dopamine receptor agonist, ADTN. *J. Med. Chem.* **1986**, *29*, 2104–2107.